

UC Santa Cruz

UC Santa Cruz Previously Published Works

Title

Measurement of the top quark pair cross section with ATLAS in pp collisions at $s=7$ TeV using final states with an electron or a muon and a hadronically decaying τ lepton

Permalink

<https://escholarship.org/uc/item/1mp1786t>

Journal

Physics Letters B, 717(1-3)

ISSN

0370-2693

Authors

Collaboration, ATLAS
Aad, G
Abbott, B
[et al.](#)

Publication Date

2012-10-01

DOI

10.1016/j.physletb.2012.09.032

Copyright Information

This work is made available under the terms of a Creative Commons Attribution License, available at <https://creativecommons.org/licenses/by/4.0/>

Peer reviewed



Measurement of the top quark pair cross section with ATLAS in pp collisions at $\sqrt{s} = 7$ TeV using final states with an electron or a muon and a hadronically decaying τ lepton[☆]

ATLAS Collaboration[☆]

ARTICLE INFO

Article history:

Received 9 May 2012

Received in revised form 21 August 2012

Accepted 8 September 2012

Available online 18 September 2012

Editor: H. Weerts

Keywords:

Top quark physics

Cross section

Lepton + τ

ABSTRACT

A measurement of the cross section of top quark pair production in proton–proton collisions recorded with the ATLAS detector at the Large Hadron Collider at a centre-of-mass energy of 7 TeV is reported. The data sample used corresponds to an integrated luminosity of 2.05 fb⁻¹. Events with an isolated electron or muon and a τ lepton decaying hadronically are used. In addition, a large missing transverse momentum and two or more energetic jets are required. At least one of the jets must be identified as originating from a b quark. The measured cross section, $\sigma_{t\bar{t}} = 186 \pm 13$ (stat.) ± 20 (syst.) ± 7 (lumi.) pb, is in good agreement with the Standard Model prediction.

© 2012 CERN. Published by Elsevier B.V. Open access under [CC BY-NC-ND license](http://creativecommons.org/licenses/by-nc-nd/3.0/).

1. Introduction

Measuring the top quark pair ($t\bar{t}$) production cross section ($\sigma_{t\bar{t}}$) in different decay channels is of interest because it can indicate physics beyond the Standard Model (SM). In the SM, the top quark decays with a branching ratio close to 100% into a W boson and a b quark, and $t\bar{t}$ pairs are identified by either the hadronic or leptonic decays of the W bosons and the presence of additional jets. The ATLAS Collaboration has previously used the single-lepton channel [1] from a 35 pb⁻¹ data sample, and the dilepton channels including only electrons and muons [2] from a 0.7 fb⁻¹ data sample, to perform cross-section measurements at 7 TeV proton–proton centre-of-mass energy. Similar measurements have been performed by the CMS Collaboration [3–5]. All these measurements are systematics limited.

The large data samples for $t\bar{t}$ production at the Large Hadron Collider (LHC) provide an opportunity to measure $\sigma_{t\bar{t}}$ using final states with an electron or a muon and a τ lepton with high precision. The $\sigma_{t\bar{t}}$ in this channel has been measured at the Tevatron in $p\bar{p}$ collisions at 1.96 TeV with 25% precision [6] and recently by the CMS Collaboration at the LHC with 18% precision [7]. A deviation from the value of $\sigma_{t\bar{t}}$ measured in other final states would be an indication of non-Standard Model decays of the top quark, such as a decay to a charged Higgs (H^+) and a b quark with H^+ decaying to a τ lepton and a τ neutrino, or of contributions from other non-Standard Model processes [8–10]. Upper limits on the

branching ratio of top quark decays to H^+ bosons decaying to a τ lepton and a neutrino have been published by Tevatron and LHC experiments [11–13].

2. Analysis overview

This analysis uses 2.05 fb⁻¹ of data collected by ATLAS from pp collisions in the LHC at a centre-of-mass energy of 7 TeV between March and August 2011. The $t\bar{t}$ events are selected with kinematic criteria that make use of the fact that they feature two W bosons and two b quarks. The selections favour events with one W decay to a charged ℓ (with ℓ denoting an electron or a muon; either prompt or from a τ lepton decay to ℓ) and a neutrino and the other W decays to a τ lepton and a neutrino with the τ lepton in turn decaying hadronically. In addition at least one jet is tagged (b -tag) as originating from a b quark (b -jet) by means of an algorithm that can identify b -jets with high efficiency while maintaining a high rejection of light-quark jets. Isolated electrons and muons are well identified, but because of the large cross section for multi-jet production the background from jets misidentified as isolated electrons or muons is not negligible. This background is reduced by requiring significant missing transverse momentum signalling the presence of energetic neutrinos. Hadronic τ lepton decays are more difficult to identify and require elaborate techniques to reject jets and electrons misidentified as a τ lepton.

Section 5 describes how the objects used in the event selection are defined. After all selections given in Section 5.2, the dominant background to the $t\bar{t} \rightarrow \ell + \tau + X$ channel is the $t\bar{t} \rightarrow \ell +$ jets channel in which the τ candidate is from jets misidentified as hadronic τ lepton decays. Therefore, τ lepton identification (τ ID) is critical

[☆] © CERN for the benefit of the ATLAS Collaboration.

* E-mail address: atlas.publications@cern.ch.

for separating signal and background. The τ ID methodology employed in this analysis exploits a multivariate technique to build a discriminant [14]. A boosted decision tree (BDT) algorithm is used [15,16]. The number of τ leptons in the selected samples is extracted by fitting the distributions of BDT outputs to background and signal templates. Section 6 describes how the background templates are constructed using control data samples. They exploit the fact that events with ℓ and τ candidates of opposite sign charge (OS) contain real τ leptons while those with same sign charge (SS) are pure background. Events with τ leptons are not all from $t\bar{t}$; the contribution from processes other than $t\bar{t} \rightarrow \ell + \tau + X$ is estimated from Monte Carlo simulation. Section 7 describes the fitting procedure and the results of the fit. The fit results are also checked using an alternative method, referred to as the “matrix method”, based on a cut on the BDT output (Section 7.1). The measured cross section is given in Section 8 and the conclusions are in Section 9.

3. ATLAS detector

The ATLAS detector [17] at the LHC covers nearly the entire solid angle around the collision point.¹ It consists of an inner tracking detector surrounded by a thin superconducting solenoid, electromagnetic (EM) and hadronic calorimeters, and an external muon spectrometer incorporating three large superconducting toroid magnet assemblies. The inner tracking detector provides tracking information in a pseudorapidity range $|\eta| < 2.5$. The liquid-argon (LAr) EM sampling calorimeters cover a range of $|\eta| < 3.2$ with fine granularity. An iron-scintillator tile calorimeter provides hadronic energy measurements in the central rapidity range ($|\eta| < 1.7$). The endcap and forward regions are instrumented with LAr calorimeters for both EM and hadronic energy measurements covering $|\eta| < 4.9$. The muon spectrometer provides precise tracking information in a range of $|\eta| < 2.7$.

ATLAS uses a three-level trigger system to select events. The level-1 trigger is implemented in hardware using a subset of detector information to reduce the event rate to below 75 kHz. This is followed by two software-based trigger levels, level-2 and the event filter, which together reduce the event rate to about 300 Hz recorded for analysis.

4. Simulated event samples

Monte Carlo (MC) simulation samples are used to optimise selection procedures, to calculate the signal acceptance and to evaluate the background contributions from single top quark, WW , WZ and ZZ production and $Z \rightarrow \tau^+\tau^-$ decays. After event generation, all samples are processed with the GEANT4 [18] simulation of the ATLAS detector, the trigger simulation and are then subject to the same reconstruction algorithms as the data [19].

For the $t\bar{t}$ and single top quark final states, the next-to-leading-order (NLO) generator MC@NLO [20–22] is used with a top quark mass of 172.5 GeV and with the NLO parton distribution function (PDF) set CTEQ6.6 [23]. The MC@NLO program uses HERWIG [24] to simulate the parton shower and hadronise the partons. The “diagram removal scheme” is used to remove overlaps between the single top quark and the $t\bar{t}$ final states. The $t\bar{t}$ cross section is normalised to the prediction of HATHOR (164_{-16}^{+11} pb) [25], which employs an approximate next-to-next-to-leading-order (NNLO) per-

turbative Quantum Chromodynamics (QCD) calculation. The diboson samples are generated with HERWIG. $W + \text{jets}$ events and $Z/\gamma^* + \text{jets}$ events (with dilepton invariant mass $m_{\ell\ell} > 40$ GeV) are generated by the ALPGEN generator [26] with up to five outgoing partons from the hard scattering process, in addition to the lepton pairs.² The MLM matching scheme [27] of the ALPGEN generator is used to remove overlaps between matrix-element and parton-shower products. Parton evolution and hadronisation is handled by HERWIG, as is the generation of diboson events. The leading-order PDF set CTEQ6L is used for all backgrounds described above.

All samples that use HERWIG for parton shower evolution and hadronisation rely on JIMMY [28] for the underlying event model. The τ -lepton decays are handled by TAUOLA [29]. The effect of multiple pp interactions per bunch crossing (“pile-up”) is modelled by overlaying simulated minimum bias events over the original hard-scattering event [30]. MC events are then reweighted so that the distribution of interactions per crossing in the MC simulation matches that observed in data. The average number of pile-up interactions in the sample is 6.3.

5. Object identification and event selection

The event selection uses nearly the same object definition as in the $t\bar{t}$ cross-section measurement in the dilepton channel [2] with the exception of a τ candidate instead of a second electron or muon candidate. The electrons must be isolated and have $E_T > 25$ GeV and $|\eta_{\text{cluster}}| < 2.47$, excluding the barrel-endcap transition region ($1.37 < |\eta_{\text{cluster}}| < 1.52$), where E_T is the transverse energy and η_{cluster} is the pseudorapidity of the calorimeter energy cluster associated with the candidate. The electron is defined as isolated if the E_T deposited in the calorimeter and not associated with the electron in a cone in η - ϕ space of radius $\Delta R = 0.2$ is less than 4 GeV. The muons must also be isolated and have transverse momentum $p_T > 20$ GeV and $|\eta| < 2.5$. For isolated muons, both the corresponding E_T and the analogous track isolation transverse momentum must be less than 4 GeV in a cone of $\Delta R = 0.3$. The track isolation p_T is calculated from the sum of the track transverse momenta for tracks with $p_T > 1$ GeV around the muon. Jets are reconstructed with the anti- k_t algorithm [31] with a radius parameter $R = 0.4$, starting from energy deposits (clusters) in the calorimeter reconstructed using the scale established using $Z \rightarrow e^+e^-$ events for electromagnetic objects. These jets are then calibrated to the hadronic energy scale using p_T - and η -dependent correction factors obtained from simulation [32]. The jet candidates are required to have $p_T > 25$ GeV and $|\eta| < 2.5$. A jet is tagged as a b -jet by a vertex tagging algorithm that constructs a likelihood ratio of b - and light-quark jet hypothesis using the following discriminating variables: the signed impact parameter significance of well measured tracks associated with a given jet, the decay length significance associated with a reconstructed secondary vertex, the invariant mass of all tracks associated to the secondary vertex, the ratio of the sum of the energies of the tracks associated with the secondary vertex to the sum of the energies of all tracks in the jet assuming a pion hypothesis, and the number of two-track vertices that can be formed at the secondary vertex. The cut on the combined likelihood ratio has been chosen to give an average efficiency of 70% for b -quark jets from $t\bar{t}$ events and a 1% efficiency for light-quark and gluon jets [33].

¹ Atlas uses a right-handed coordinate system with its origin at the nominal interaction point in the centre of the detector and the z -axis along the beam pipe. The x -axis points to the centre of the LHC ring, and the y -axis points upwards. The azimuthal angle ϕ is measured around the beam axis and the polar angle θ is the angle from the beam axis. The pseudorapidity is defined as $\eta = -\ln[\tan(\theta/2)]$. The distance ΔR in η - ϕ space is defined as $\Delta R = \sqrt{(\Delta\phi)^2 + (\Delta\eta)^2}$.

² The fraction of events with $m_{\ell\ell} < 40$ GeV is estimated to be less than 0.2% of the total after all selections. The estimate is based on ALPGEN samples for Drell–Yan simulation and confirmed by a good agreement with data.

The missing transverse momentum is constructed from the vector sum of all calorimeter cells with $|\eta| < 4.5$, projected onto the transverse plane. Its magnitude is denoted E_T^{miss} . The hadronic energy scale is used for the energies of cells associated with jets; τ candidates are treated as jets. Contributions from cells associated with electrons employ the electromagnetic energy calibration. Contributions from the p_T of muon tracks are included, removing the contributions of any calorimeter cells associated with the muon.

5.1. τ reconstruction and identification

The reconstruction and identification of hadronically decaying τ leptons proceed as follows:

1. the τ candidate reconstruction starts by considering each jet as a τ candidate;
2. energy clusters in the calorimeter associated with the τ candidate are used to calculate kinematic quantities (such as E_T) and the associated tracks are found;
3. identification variables are calculated from the tracking and calorimeter information;
4. these variables are combined into multivariate discriminants and the outputs of the discriminants are used to separate jets and electrons misidentified as τ leptons decaying hadronically from τ leptons.

Details, including the variable definitions used in the multivariate discriminants, are given in Ref. [9]. In this analysis the outputs of BDT discriminants are used.

Reconstructed τ candidates are required to have $20 \text{ GeV} < E_T < 100 \text{ GeV}$. They must also have $|\eta| < 2.3$, and one, two or three associated tracks. A track is associated with the τ candidate if it has $p_T > 1 \text{ GeV}$ and is inside a cone of $\Delta R < 0.4$ around the jet axis. The associated track with highest p_T must have $p_T > 4 \text{ GeV}$. The charge is given by the sum of the charges of the associated tracks, and is required to be non-zero. The probability of misidentifying the τ lepton charge sign is about 1%. The charge misidentification rate for muons and electrons is negligible.

If the τ candidate overlaps with a muon (with $p_T > 4 \text{ GeV}$ and without an isolation requirement) or an electron candidate within $\Delta R(\ell, \tau) < 0.4$, the τ candidate is removed. To remove electrons misidentified as τ leptons, an additional criterion is used that relies on a BDT trained to separate τ leptons and electrons (BDT_e) using seven variables shown to be well modelled by comparing $Z \rightarrow e^+e^-$ and $Z \rightarrow \tau^+\tau^-$ events in data and in MC simulation. The variables were chosen after ranking a large set by their effectiveness.³ The most effective variables for BDT_e are E/p , the EM fraction (the ratio of the τ candidate energy measured in the EM calorimeter to the total τ candidate energy measured in the calorimeter), and the cluster-based shower width. The BDT output tends to be near 1 (0) if the τ candidate is a τ lepton (electron). BDT_e was trained using $Z \rightarrow e^+e^-$ and $Z \rightarrow \tau^+\tau^-$ Monte Carlo samples. The τ candidate is required to satisfy $\text{BDT}_e > 0.51$; 85% of reconstructed τ leptons decaying hadronically satisfy this requirement, as measured in $Z \rightarrow \tau^+\tau^-$ events. The additional rejection for electrons is a factor of 60.

The majority of objects reconstructed as τ candidates in a multi-jet environment are jets misidentified as τ leptons. A jet or an electron misidentified as a τ lepton will be referred to as

a fake τ . Another BDT (BDT_j) based on eight variables is used to separate τ leptons in τ candidates with one track (denoted τ_1) from such jets. For candidates with more than one track (denoted τ_3) BDT_j includes ten variables. The BDT_j was trained using multi-jet events as background and $Z \rightarrow \tau^+\tau^-$ Monte Carlo as signal. The most effective variables for BDT_j are calorimeter and track isolation, cluster-based jet mass, and the fraction of energy within $\Delta R = 0.1$ of the jet axis. The BDT_j distributions are fit with templates for background and signal to extract the number of τ leptons in the sample. Details are given in Section 7. The fake τ background in the τ_3 sample is significantly higher than in the τ_1 sample, leading to very different BDT_j distributions. Hence independent measurements are carried out for τ_1 and τ_3 candidate events and the results are combined at the end. If there is a τ_1 and a τ_3 candidate in the event, the τ_1 candidate is kept as the probability that the τ_1 is a τ lepton is much higher. If there are two τ_1 or τ_3 candidates, both are kept.

5.2. Event selection

For this analysis, events are selected using a single-muon trigger with a p_T threshold of 18 GeV or a single-electron trigger with a p_T threshold of 20 GeV, rising to 22 GeV during periods of high instantaneous luminosity. The offline requirements are based on data quality criteria and optimised using Monte Carlo simulation:

- a primary vertex with at least five tracks, each with $p_T > 400 \text{ MeV}$, associated with it;
- one and only one isolated high- p_T muon and no identified electrons for the $\mu + \tau$ channel, or one and only one isolated electron and no isolated muons for the $e + \tau$ channel;
- at least one τ candidate (as defined in Section 5.1);
- at least two jets not overlapping with a τ candidate, i.e. $\Delta R(\tau, \text{jet}) > 0.4$;
- $E_T^{\text{miss}} > 30 \text{ GeV}$ to reduce the multi-jet background, and the scalar sum of the p_T of the leptons (including τ), jets, and E_T^{miss} must be greater than 200 GeV, to reduce the $W + \text{jets}$ background.

The $\ell + \tau$ samples are divided into events with no jets identified as a b -quark jet (0 b -tag control sample) and those with at least one such jet (≥ 1 b -tag $t\bar{t}$ sample). The 0 b -tag sample is used to estimate the background in the ≥ 1 b -tag $t\bar{t}$ sample. Each sample is split into two, one with the τ candidate and ℓ having the opposite sign charge (OS), and the other one with τ and ℓ having the same sign charge (SS). While the τ candidates in the SS samples are almost all fake τ leptons, the OS samples have a mixture of τ leptons and fake τ leptons. The numbers of observed and expected events in the above samples are shown in Table 1. The $\ell + \text{jets}$ entry is the contribution from all processes with a ℓ and a τ candidate that is a jet misidentified as a τ lepton other than from $t\bar{t}$ ($\rightarrow \ell + \text{jets}$). The τ entries require the reconstructed τ candidate be matched to a generated τ lepton. The matching criterion is $\Delta R < 0.1$ between the τ candidate and the observable component of the generated τ lepton.

To estimate the multi-jet background from data, an event selection identical to the $\mu + \tau$ ($e + \tau$) event selection except for an inverted muon (electron) isolation cut is used to obtain a multi-jet template for the shape of the transverse mass, $m_T = \sqrt{(E_T^\ell + E_T^{\text{miss}})^2 - (p_x^\ell + E_x^{\text{miss}})^2 - (p_y^\ell + E_y^{\text{miss}})^2}$. The normalisation of each selected data sample is obtained by fitting the m_T distribution of the selected data samples with the multi-jet template and the sum of non-multi-jet processes predicted by MC, allowing the amount of both to float. The uncertainty on the multi-jet

³ The effectiveness is quantified by quadratically summing over the change in the purity between the mother and daughter leaves for every node in which the given variable is used in a decision tree.

Table 1
Number of $\ell + \tau$ candidates for Monte Carlo samples and data. $t\bar{t}(\ell + e)$ are $t\bar{t}$ events with one identified lepton and an electron reconstructed as a τ candidate. $t\bar{t}(\ell + \text{jets})$ are $t\bar{t}$ events with one identified lepton and a jet reconstructed as a τ candidate. $\ell + \text{jets}$ are events with one identified lepton and a jet reconstructed as a τ candidate from sources other than $t\bar{t}(\ell + \text{jets})$ and multi-jets. Sources contributing to jet fakes are $W + \text{jets}$, $Z + \text{jets}$, single top quark, diboson events and $t\bar{t}$. $Wt(\ell + \tau)$ is $W + t$ production with one W decaying to ℓ and another to τ . The uncertainties are statistical only, except for the multi-jet estimates. MC samples are normalised to the data integrated luminosity.

$\mu + \tau$	τ_1				τ_3			
	0 b -tag		≥ 1 b -tag		0 b -tag		≥ 1 b -tag	
	OS	SS	OS	SS	OS	SS	OS	SS
$t\bar{t}(\mu + \tau)$	60 ± 2	<1	390 ± 4	2 ± 1	17 ± 1	1 ± 1	118 ± 3	2 ± 1
$t\bar{t}(\mu + e)$	3 ± 1	<1	12 ± 1	1 ± 1	1 ± 1	<1	3 ± 1	<1
$t\bar{t}(\mu + \text{jets})$	308 ± 4	163 ± 3	1528 ± 9	660 ± 6	685 ± 6	443 ± 5	3484 ± 13	2000 ± 10
$\mu + \text{jets}$	5010 ± 70	3020 ± 60	496 ± 17	297 ± 13	12230 ± 120	8670 ± 90	1293 ± 28	928 ± 24
Multi-jets	470 ± 140	540 ± 160	117 ± 35	150 ± 40	990 ± 300	1120 ± 340	460 ± 140	400 ± 120
$Wt(\mu + \tau)$	7 ± 1	<1	18 ± 1	1 ± 1	2 ± 1	<1	5 ± 1	<1
$Z \rightarrow \tau\tau$	301 ± 13	2 ± 1	16 ± 3	<1	75 ± 7	1 ± 1	3 ± 2	<1
Total	6160 ± 160	3730 ± 170	2580 ± 40	1110 ± 40	14000 ± 320	10230 ± 350	5370 ± 140	3330 ± 120
Data	5450	3700	2472	1332	13322	10193	5703	3683

$e + \tau$	τ_1				τ_3			
	0 b -tag		≥ 1 b -tag		0 b -tag		≥ 1 b -tag	
	OS	SS	OS	SS	OS	SS	OS	SS
$t\bar{t}(e + \tau)$	54 ± 7	1 ± 1	342 ± 19	3 ± 2	15 ± 4	<1	103 ± 10	2 ± 1
$t\bar{t}(e + e)$	2 ± 1	<1	11 ± 3	1 ± 1	<1	<1	2 ± 1	<1
$t\bar{t}(e + \text{jets})$	273 ± 17	146 ± 12	1340 ± 40	599 ± 25	633 ± 25	399 ± 20	3090 ± 60	1780 ± 40
$e + \text{jets}$	3950 ± 60	2590 ± 50	380 ± 20	256 ± 16	10140 ± 100	7530 ± 90	1120 ± 33	841 ± 29
Multi-jets	600 ± 180	620 ± 190	170 ± 50	140 ± 40	2000 ± 600	2000 ± 600	690 ± 210	610 ± 180
$Z \rightarrow ee$	92 ± 10	3 ± 2	9 ± 3	<1	11 ± 3	2 ± 1	<1	<1
$Wt(e + \tau)$	7 ± 3	<1	17 ± 4	<1	1 ± 1	<1	5 ± 2	<1
$Z \rightarrow \tau\tau$	217 ± 15	2 ± 1	15 ± 4	<1	60 ± 7	1 ± 1	3 ± 2	<1
Total	5190 ± 190	3360 ± 200	2280 ± 70	990 ± 50	12900 ± 600	9900 ± 600	5020 ± 220	3230 ± 180
Data	5111	3462	2277	1107	12102	9635	5033	3192

background is estimated to be 30%. This estimate is only used to illustrate the background composition. The background models are derived from data (see Section 6) and do not depend on knowing the exact composition. All processes contribute more events to OS than SS because of the correlation between a leading-quark charge and the lepton charge, except for the multi-jet channel contribution which within uncertainties has equal numbers of OS and SS events. As one can see from Table 1, the τ leptons are almost all in the OS sample and come mainly from two sources: $Z \rightarrow \tau^+\tau^-$, which is the dominant source in the sample with 0 b -tag, and $t\bar{t} \rightarrow \ell + \tau + X$ which is the dominant source in the sample ≥ 1 b -tag. The sources of fake τ leptons are quite distinct between the 0 b -tag and the ≥ 1 b -tag samples: the first is mainly $W/Z + \text{jets}$ with small contributions from other channels, the second is mainly $t\bar{t}$.

6. Background models

The jet origin can strongly influence the τ -lepton fake probability. Due to their narrow shower width and lower track multiplicity, light-quark jets have a higher probability of faking a τ lepton than other jet types. Thus the BDT_j distributions have a strong dependence on the jet type. It is therefore crucial to build a background model which properly reflects the jet composition in order to correctly estimate the fake τ contamination in the signal region. Deriving this background model from control regions in data rather than MC simulation is preferable in order to avoid systematic effects related to jet composition in the MC models.

The gluon component of the fake τ leptons is charge symmetric; therefore it is expected to have the same shape in SS events as in OS events and should contribute the same number of fake τ leptons in each sample. The contribution of fake τ leptons from gluons can be removed by subtracting the distribution of any quantity for SS events from the corresponding distribution for OS events.

The multi-jet background also cancels, as can be seen in Table 1. The resulting distributions are labelled OS-SS. Similarly, since each sample is expected to have an almost equal contribution from b -jets and \bar{b} -jets, the small b -jet component should also be removed by OS-SS (the asymmetry in b production, mainly from single top quark final states, is negligible). The only jet types remaining in the OS-SS distributions are light-quark jets. MC studies indicate that the BDT_j distributions of c -quark jets misidentified as τ leptons are not noticeably different from those of light-quark jets.

One can construct a background BDT_j distribution from the 0 b -tag data sample by subtracting the expected amount of τ -lepton signal. The signal is mainly from $Z \rightarrow \tau^+\tau^-$ and can be reliably predicted from MC. A control sample dominated by $W + \text{jets}$ events is considered as a check. The latter sample is selected by requiring events with a muon and a τ candidate, no additional jets, $E_T^{\text{miss}} > 30$ GeV and $40 \text{ GeV} < m_T < 100$ GeV. According to MC simulation, in $W + \text{jets}$ events where exactly one jet is required, 90% of the fake τ leptons are from light-quark jets and 10% from gluons. This sample is labelled $W + 1$ jet.

The BDT_j background shapes for the OS-SS 0 b -tag and ≥ 1 b -tag data samples are not identical to the $W + 1$ jet distributions for two reasons: (1) the shape depends on the jet multiplicity, (2) different OS/SS ratios are observed in the samples. The dependence on the OS/SS ratio comes from the differences in jet fragmentation producing a leading particle with the opposite charge and the same charge as the initial quark; thus the OS BDT_j shape from light-quark jets differs from the equivalent SS BDT_j shape. The ratio of OS-SS BDT_j background distributions derived from $W + 1$ jet and ≥ 1 b -tag simulated events show that significant corrections are needed (30% for $\text{BDT}_j > 0.8$, a region dominated by the true τ signal). For the 0 b -tag sample the corresponding corrections are much smaller (5% in the same region). Both the 0 b -tag and the $W + 1$ jet data samples are used to obtain statistically independent estimates of the background in the ≥ 1 b -tag sample.

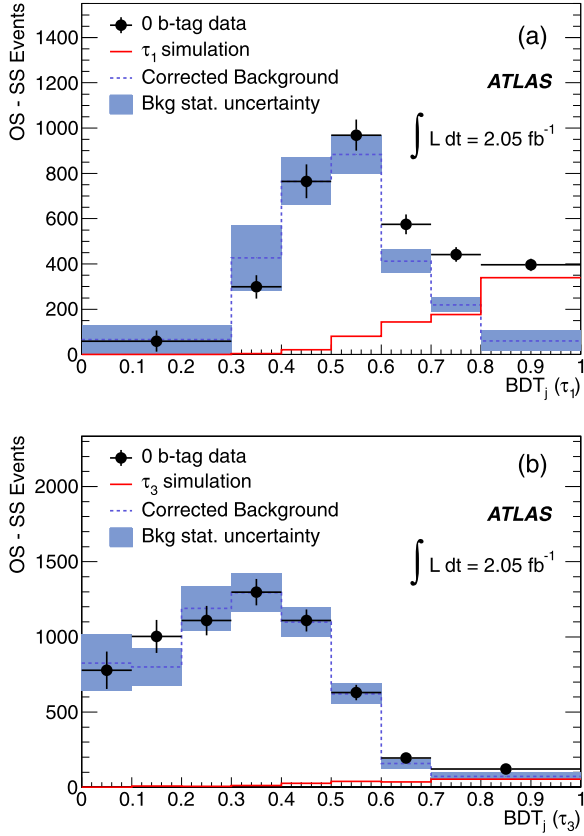


Fig. 1. BDT_j (OS-SS) distributions of $\ell + \tau$ (e and μ combined) events in the 0 b -tag data (black points): (a) τ_1 , (b) τ_3 . The expected contributions from τ and e (sum of $Z \rightarrow \tau^+\tau^-$, single top and $t\bar{t} \rightarrow \ell + \tau + X$) are shown as a solid red line. The derived background templates after applying MC corrections are shown as dashed histogram with shaded/blue statistical uncertainty bands. The shapes of these background templates are used for the fits to the ≥ 1 b -tag distributions.

Two different approaches are used for constructing backgrounds in the ≥ 1 b -tag data sample. One, used by the fit method (Section 7), is to reweight the BDT_j distribution of the background bin-by-bin using the MC-based ratio of the ≥ 1 b -tag background to the background model. In this case the 0 b -tag sample is preferred as it requires smaller corrections derived from MC simulation; the $W + 1$ jet is used as a cross check. The other approach is to split the background into bins of some variable within which the shapes of BDT_j distributions of the background model are close to those from the ≥ 1 b -tag background. This approach, used in the matrix method cross check (Section 7.1), avoids using MC corrections, but assumes the data and MC simulation behave similarly as function of the binning variable.

7. Fits to BDT_j distributions

The contribution from $t\bar{t} \rightarrow \ell + \tau + X$ signal is derived from the ≥ 1 b -tag data sample by a χ^2 fit to the OS-SS BDT_j distribution with a background template and a signal template. The parameters of the fit are the amount of background and the amount of signal. The shapes of the templates are fixed.

Two statistically independent background templates corrected by MC, as discussed in Section 6, are used: one derived from 0 b -tag data, the other (purely as a check) derived from the $W + 1$ jet data sample. The signal BDT_j templates for 0 b -tag and ≥ 1 b -tag are derived from τ leptons in $t\bar{t}$ and $Z \rightarrow \tau^+\tau^-$ MC simulation. Contributions to the BDT_j distributions from electrons passing the BDT_e cut cannot be distinguished from τ leptons so they are treated as part of the signal.

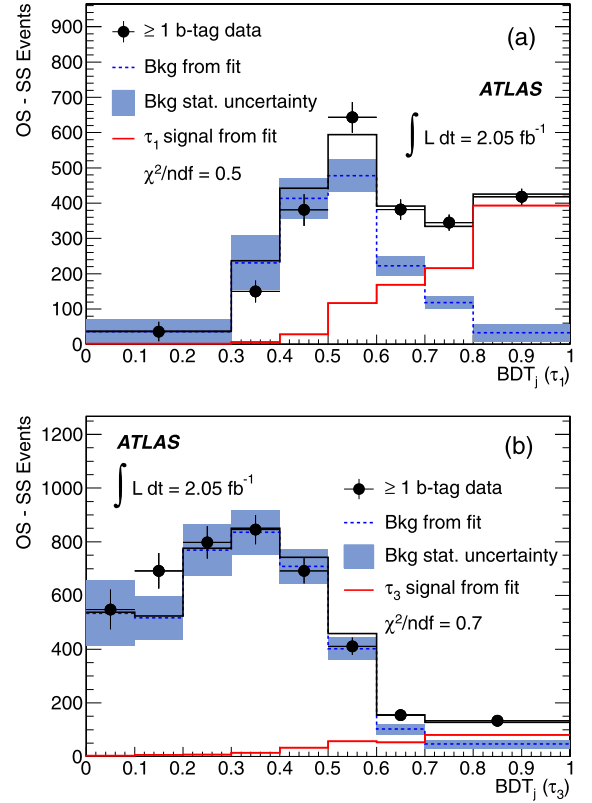


Fig. 2. BDT_j (OS-SS) distributions of $\ell + \tau$ in the ≥ 1 b -tag sample; (a) τ_1 , (b) τ_3 . The normalisation of each template is derived from a fit to the data. The fitted contributions are shown as the light/red (signal), dashed/blue (background derived from 0 b -tag after applying MC corrections) and dark/black (total) lines. Shaded/blue bands are the statistical uncertainty of the background template.

The uncertainty on the background templates is determined by the numbers of data and MC simulated events. The signal template for the 0 b -tag control sample has a non-negligible statistical uncertainty (2% for τ_1 , 5% for τ_3) because of the low acceptance.

The fitting procedure was tested extensively with MC simulation before applying it to data. In the fits to the ≥ 1 b -tag data, applying MC corrections to the 0 b -tag background template increases the statistical uncertainty because of the uncertainty due to the number of simulated events but raises the measured cross section by only 1%.

Fig. 1 shows the BDT_j (OS-SS) distributions of $\ell + \tau$ events with 0 b -tag and the 0 b -tag background template after subtracting the expected number of τ leptons and applying the MC corrections. The τ signal is mostly $Z \rightarrow \tau^+\tau^-$ events with a small contamination of electrons faking τ leptons (from $t\bar{t} \rightarrow \ell + e + X$ and $Z \rightarrow e^+e^-$) and a small contribution from $t\bar{t} \rightarrow \ell + \tau + X$. The uncertainty on the background template includes the statistical uncertainty of the correction, the statistical uncertainty from MC and the 0 b -tag data uncertainty.

Fig. 2 shows the result of the fit to the ≥ 1 b -tag samples. The τ lepton signal is mostly $t\bar{t} \rightarrow \ell + \tau + X$ with a small contamination of misidentified electrons (estimated by applying fake probabilities derived from data), and small contributions from $Z \rightarrow \tau^+\tau^-$ events and single top quark events (estimated from MC simulation). These contributions are subtracted from the number of fitted τ lepton signal events before calculating the cross section. The fit results using the background templates derived from 0 b -tag data and $W + 1$ jet data are shown in Table 2. The results are consistent with each other within the statistical uncertainties of the background templates. The BDT_j distributions for τ_1 and τ_3 are

Table 2

Results of template fits to $\mu + \tau$, $e + \tau$ and the combined BDT_j distributions. The combined results are obtained by fitting the sum of the $\mu + \tau$ and $e + \tau$ BDT_j distributions. The first column gives the channel and the second the τ type. The third column shows the extracted signal (sum of τ leptons and electrons misidentified as τ leptons) with the background template derived from 0 b -tag data distributions. The fourth column shows the extracted signal with the background template derived from $W + 1$ jet. The uncertainties are from the uncertainties in the fit parameters and do not include the systematic uncertainties. The MC columns give the expected τ signal (includes the contribution of non- $t\bar{t} \rightarrow l + \tau$ events) and the expected number of $t\bar{t} \rightarrow l + \tau$ assuming the theoretical $t\bar{t}$ production cross section (164 pb).

		Background template		MC	
		0 b -tag	$W + 1$ jet	Signal	$t\bar{t}$
$\mu + \tau$	τ_1	490 ± 40	456 ± 32	432	388
	τ_3	135 ± 33	130 ± 50	126	116
$e + \tau$	τ_1	440 ± 50	430 ± 50	388	338
	τ_3	116 ± 32	120 ± 28	114	101
Combined	τ_1	930 ± 70	860 ± 50	820	726
	τ_3	260 ± 60	260 ± 40	239	217

fitted separately. The combined $\ell + \tau_i$ results are obtained by fitting the sum of the distributions. After adding $\ell + \tau_1$ and $\ell + \tau_3$ signals obtained from a χ^2 fit to the combined $e + \tau$ and $\mu + \tau$ distributions and subtracting the small contributions to the signal from $Z \rightarrow \tau^+\tau^-$, $Z \rightarrow e^+e^-$ and $t\bar{t} \rightarrow e + \ell$ (given in Table 1), the results are 840 ± 70 (243 ± 60) $t\bar{t} \rightarrow \ell + \tau_1(\tau_3) + X$ events. The uncertainty is from the fit only and does not include systematic uncertainties. The results are in good agreement with the 780 ± 50 (243 ± 60) events obtained with the $W + 1$ jet background template and consistent with the number expected from MC simulation, 726 ± 19 (217 ± 10). Note that the fit uncertainty is dominated by the uncertainties on the background template, thus the statistical uncertainties of the results with the two different background templates are not strongly correlated.

Fig. 3 shows the OS-SS distribution of the number of jets for ≥ 1 b -tag events adding all channels for two BDT_j regions: $\text{BDT}_j < 0.7$, which is dominated by $t\bar{t} \rightarrow \ell + \tau$ and jets, and $\text{BDT}_j > 0.7$, in which the largest contribution is from $t\bar{t} \rightarrow \ell + \tau + X$. As expected, the multiplicity of jets peaks at four when $\text{BDT}_j < 0.7$ and three when $\text{BDT}_j > 0.7$ (the τ is counted as a jet). Fig. 4 shows the invariant mass of a selected jet with the τ candidate for $\text{BDT}_j < 0.7$ and $\text{BDT}_j > 0.7$ for events with a τ candidate and three or more jets. The selected jet is the highest p_T untagged jet in events with more than one b -tag and the second highest p_T untagged jet in events with one b -tag. The distribution shows clearly the presence of a W decaying to two jets in the $\text{BDT}_j < 0.7$ region dominated by $t\bar{t} \rightarrow \ell + \tau$ and jets. The mass distribution in the $\text{BDT}_j > 0.7$ signal region is significantly broader as expected for $t\bar{t} \rightarrow \ell + \tau + X$. The signal and background shown in these figures are based on the fit using the 0 b -tag background template.

7.1. Check with matrix method

From Figs. 3 and 4 one can see that a $\text{BDT}_j > 0.7$ requirement separates well a region dominated by $t\bar{t} \rightarrow \ell + \tau$ and jets from a region dominated by $t\bar{t} \rightarrow \ell + \tau + X$. One can extract the signal from the same OS-SS ≥ 1 b -tag sample used by the fit method via a matrix method. All τ candidates are labelled “loose”, and τ candidates with $\text{BDT}_j > 0.7$ are labelled “tight”. The probability that the loose τ candidates are also tight τ candidates, for both τ leptons and fake τ leptons, is defined as

$$\epsilon_{\text{real}} = \frac{N_{\text{real}}^{\text{tight}}}{N_{\text{real}}^{\text{loose}}} \quad \epsilon_{\text{fake}} = \frac{N_{\text{fake}}^{\text{tight}}}{N_{\text{fake}}^{\text{loose}}}$$

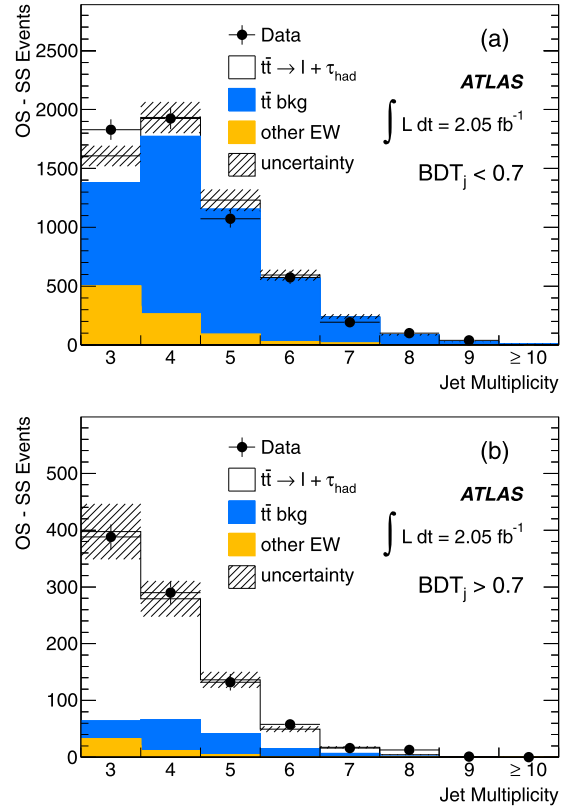


Fig. 3. OS-SS number of jets distributions for events with at least one b -tag. The $\mu + \tau$ and $e + \tau$ channels have been summed together. The solid circles indicate data and the histograms indicate the expected signal and backgrounds. The normalisation of the expected signal and the backgrounds are based on the fit result. The uncertainty includes statistical and systematic contributions. The fraction of each background is estimated from MC. (a) is for $\text{BDT}_j < 0.7$, (b) for $\text{BDT}_j > 0.7$.

where the “real” subscript denotes τ lepton, the “fake” subscript denotes fake τ and N is the number of τ candidates. The number of “tight” τ leptons is then given by

$$N_{\text{real}}^{\text{tight}} = N_{\text{data}}^{\text{tight}} - \frac{\epsilon_{\text{fake}}}{\epsilon_{\text{real}} - \epsilon_{\text{fake}}} (N_{\text{data}}^{\text{loose}} \cdot \epsilon_{\text{real}} - N_{\text{data}}^{\text{tight}}).$$

The value of ϵ_{fake} is measured utilising the OS-SS BDT_j distributions from the background control samples; ϵ_{real} is derived from MC (including all processes that contribute a τ lepton or an electron misidentified as a τ lepton) and was tested using $Z \rightarrow \tau^+\tau^-$ events. This method uses the binning approach described in Section 6 to estimate the background. Values of ϵ_{fake} and ϵ_{real} are measured separately for three EM-fraction bins. The EM-fraction, the ratio of the energy measured in the EM calorimeter to the total τ candidate energy measured in the calorimeter, is an effective variable for splitting the data into regions where the shapes of MC OS-SS BDT_j distributions for the $W + 1$ jet background template and the ≥ 1 b -tag background are similar. Table 3 shows the number of signal events obtained with the matrix method using the background derived from the 0 b -tag data sample and from the $W + 1$ jet data sample. The numbers in each pair are in good agreement and consistent with the numbers obtained by fitting the OS-SS BDT_j distributions.

7.2. Systematic uncertainty

Several experimental and theoretical sources of systematic uncertainty are considered. Lepton trigger, reconstruction and selection efficiencies are assessed by comparing the $Z \rightarrow \ell^+\ell^-$ events

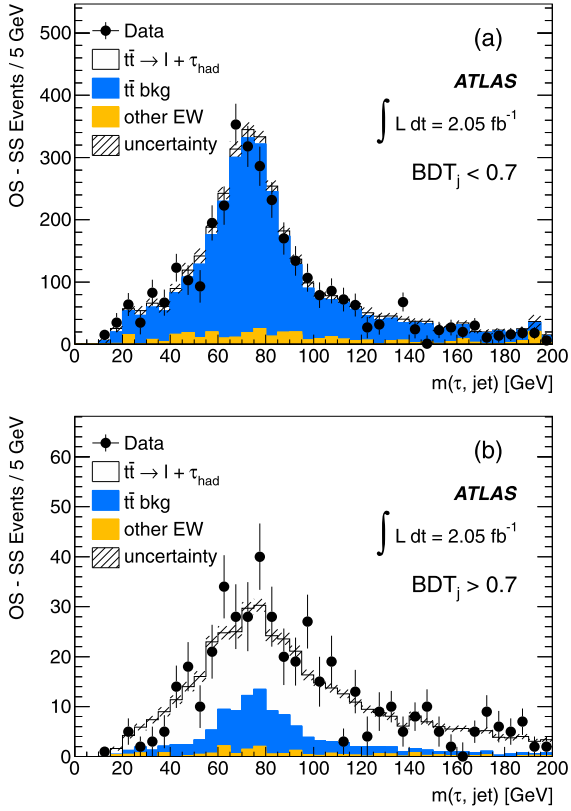


Fig. 4. OS-SS invariant mass of jet and τ candidate for events with at least one b -tag. The jet is the highest p_T untagged jet in events with more than one b -tag and the second highest p_T untagged jet in events with one b -tag. The $\mu + \tau$ and $e + \tau$ channels have been summed together. The solid circles indicate data and the histograms indicate the expected signal and backgrounds. The normalisation of the expected signal and the backgrounds are based on the fit result. The uncertainty includes statistical and systematic contributions. The fraction of each background is estimated from MC. (a) is for $BDT_j < 0.7$, (b) for $BDT_j > 0.7$.

Table 3

Number of signal events obtained with the matrix method for $\mu + \tau$, $e + \tau$ and the combined channels. The first column gives the channel and the second the τ type. The third column shows the extracted signal with the background template derived from 0 b -tag data distributions. The fourth column shows the extracted signal with the background template derived from $W + 1$ jet. In order to compare the matrix method results to the fit results the number of signal events shown is $\sum N_{\text{tight}}^{\text{real}} / \bar{\epsilon}_{\text{real}}$ where $\bar{\epsilon}_{\text{real}}$ is the ϵ_{real} averaged over the three EM-fraction bins. The uncertainties are statistical only.

		Background template	
		0 b -tag	$W + 1$ jet
$\mu + \tau$	τ_1	460 ± 50	440 ± 50
	τ_3	130 ± 40	105 ± 35
$e + \tau$	τ_1	420 ± 60	350 ± 50
	τ_3	140 ± 40	160 ± 40
Combined	τ_1	880 ± 70	800 ± 70
	τ_3	270 ± 60	260 ± 60

selected with the same object criteria as used for the $t\bar{t}$ analysis in data and MC.

Scale factors are applied to $Z \rightarrow \tau^+\tau^-$ MC samples when calculating acceptances to account for any differences between predicted and observed efficiencies. The scale factors are evaluated by comparing the observed efficiencies with those determined with simulated Z boson events. Systematic uncertainties on these scale factors are evaluated by varying the selection of events used in the

Table 4

Relative systematic uncertainties, in %, for the cross-section measurement. The first column gives the source of systematic uncertainty, ID/Trigger stands for the combined uncertainty of lepton identification and lepton trigger. The τ ID uncertainty includes electrons misidentified as τ leptons. The second and third columns give the channel.

Source	$\mu + \tau$	$e + \tau$
μ (ID/Trigger)	$-1.1 / +1.5$	–
e (ID/Trigger)	–	± 2.9
JES	$-2.0 / +2.2$	$-1.9 / +2.8$
JER	± 1.0	± 1.2
ISR/FSR	± 4.8	± 3.5
Generator	± 0.7	± 0.7
PDF	± 2.0	± 2.1
b -tag	$-7.7 / +9.0$	$-7.5 / +8.9$
τ_1 ID	$-3.0 / +3.2$	$-2.7 / +3.0$
τ_3 ID	$-3.1 / +3.4$	$-2.9 / +3.2$

efficiency measurements and by checking the stability of the measurements over the course of data taking.

The modelling of the lepton momentum scale and resolution is studied using reconstructed invariant mass distributions of $Z \rightarrow \ell^+\ell^-$ candidate events and used to adjust the simulation accordingly [34,35].

The jet energy scale (JES) and its uncertainty are derived by combining information from test-beam data, LHC collision data and simulation [32]. For jets within the acceptance, the JES uncertainty varies in the range 4–8% as a function of jet p_T and η . Comparing MC and data the estimated systematic uncertainties are 10% and 1–2% for the jet energy resolution (JER) and the jet reconstruction efficiency, respectively. The uncertainty on the efficiency of the b -tagging algorithm has been estimated to be 6% for b -quark jets, based on b -tagging calibration studies [33].

The uncertainty in the kinematic distributions of the $t\bar{t}$ signal events gives rise to systematic uncertainties in the signal acceptance, with contributions from the choice of generator, the modelling of initial- and final-state radiation (ISR/FSR) and the choice of the PDF set. The generator uncertainty is evaluated by comparing the MC@NLO predictions with those of POWHEG [36–38] interfaced to either HERWIG or PYTHIA. The uncertainty due to ISR/FSR is evaluated using the ACERMC generator [39] (which relies on the MADGRAPH package [40]) interfaced to the PYTHIA shower model, and by varying the parameters controlling ISR and FSR in a range consistent with experimental data [19]. Finally, the PDF uncertainty is evaluated using a range of current PDF sets: NNPDF, CTEQ, and MSTW [41–43]. Each one comes with a set of error PDFs, the RMS of the variations was taken as the PDF uncertainty. The dominant uncertainty in this category of systematic uncertainties is the modelling of ISR/FSR.

The τ ID uncertainty is derived from a template fit to a $Z \rightarrow \tau^+\tau^-$ data sample selected with the same μ and τ candidate requirements as the sample for this analysis, but with fewer than two jets and $m_T < 20$ GeV to remove $W + \text{jets}$ events. The fit relies on the $W + 1$ jet data sample for a background template and $Z \rightarrow \tau^+\tau^-$ MC events for a signal template. The uncertainty includes the statistical uncertainty of the data samples, the uncertainty in the Z/γ^* cross section measured by ATLAS [44] (excluding the luminosity uncertainty) and the jet energy scale uncertainty. It also includes the uncertainty on the number of misidentified electrons ($< 0.5\%$, determined from $Z \rightarrow e^+e^-$ data).

The effect of these variations on the final result is evaluated by varying each source of systematic uncertainty by $\pm 1\sigma$, applying the selection criteria to obtain new signal and background templates and recalculating the cross section.

Table 5

Measured cross section from the τ_1 and τ_3 samples, as well as the combination ($\tau_1 + \tau_3$) for each channel separately. The uncertainty in the integrated luminosity (3.7%) is not included.

	$\mu + \tau$
τ_1	189 ± 16 (stat.) ± 20 (syst.) pb
τ_3	180 ± 40 (stat.) ± 21 (syst.) pb
$\tau_1 + \tau_3$	186 ± 15 (stat.) ± 20 (syst.) pb
	$e + \tau$
τ_1	190 ± 20 (stat.) ± 20 (syst.) pb
τ_3	170 ± 50 (stat.) ± 21 (syst.) pb
$\tau_1 + \tau_3$	187 ± 18 (stat.) ± 20 (syst.) pb

The uncertainties obtained for the fit method using the 0 b -tag background template are shown in Table 4. The systematic uncertainties for the matrix method are very similar. The uncertainty on the measured integrated luminosity is 3.7% [45]. This translates into a 3.5% uncertainty on the cross section.

8. Measuring the $t\bar{t}$ cross section

The cross section is derived from the number of observed OS-SS signal events in the ≥ 1 b -tag data sample assuming the only top quark decay mode is $t \rightarrow Wb$, and subtracting from that number the small contribution from $t\bar{t} \rightarrow e + \ell$ (from electrons faking τ leptons) and τ leptons from $Z \rightarrow \tau^+\tau^-$ (Table 1). The systematic uncertainties are estimated as the quadratic sum of all uncertainties given in Table 4, which includes the uncertainty from the subtraction.

The results are given separately for τ_1 and τ_3 and then combined (weighted by their statistical uncertainty and assuming all systematic uncertainties other than from τ ID are fully correlated). The results using the 0 b -tag background template are shown in Table 5.

The results for the $\mu + \tau$ and $e + \tau$ channels are combined taking into account the correlated uncertainties using the BLUE (Best Linear Unbiased Estimator) technique [46]. Combining them does not improve the systematic uncertainty as the systematic uncertainties are almost 100% correlated.

The results for each lepton type are:

$$\mu + \tau: \quad \sigma_{t\bar{t}} = 186 \pm 15 \text{ (stat.)} \pm 20 \text{ (syst.)} \pm 7 \text{ (lumi.) pb,}$$

$$e + \tau: \quad \sigma_{t\bar{t}} = 187 \pm 18 \text{ (stat.)} \pm 20 \text{ (syst.)} \pm 7 \text{ (lumi.) pb,}$$

Combining both channels one obtains:

$$\sigma_{t\bar{t}} = 186 \pm 13 \text{ (stat.)} \pm 20 \text{ (syst.)} \pm 7 \text{ (lumi.) pb.}$$

To check the fit measurements, the cross sections can be calculated using the matrix method and the results obtained with the $W + 1$ jet background to minimise the correlation with the fit results. The combination of the matrix method and the fit results with the BLUE method shows they are compatible at the 45% and 10% confidence level for $\mu + \tau$ and $e + \tau$, respectively.

9. Conclusions

The cross section for $t\bar{t}$ production in pp collisions at 7 TeV has been measured in the $\mu + \tau$ and the $e + \tau$ channels in which the τ decays hadronically. The number of τ leptons in these channels has been extracted using multivariate discriminators to separate τ leptons from electrons and jets misidentified as hadronically decaying τ leptons. These numbers were obtained by fitting the discriminator outputs and checked with a matrix method. Combining the measurements from $\mu + \tau$ and $e + \tau$ events, the cross

section is measured to be

$$\sigma_{t\bar{t}} = 186 \pm 13 \text{ (stat.)} \pm 20 \text{ (syst.)} \pm 7 \text{ (lumi.) pb,}$$

in good agreement with the cross section measured by ATLAS in other channels [1,2], with the cross-section measurements by the CMS Collaboration [3–5,7] and with the SM prediction, 164_{-16}^{+11} pb [25].

Acknowledgements

We thank CERN for the very successful operation of the LHC, as well as the support staff from our institutions without whom ATLAS could not be operated efficiently.

We acknowledge the support of ANPCyT, Argentina; YerPhI, Armenia; ARC, Australia; BMWF, Austria; ANAS, Azerbaijan; SSTC, Belarus; CNPq and FAPESP, Brazil; NSERC, NRC and CFI, Canada; CERN; CONICYT, Chile; CAS, MOST and NSFC, China; COLCIENCIAS, Colombia; MSMT CR, MPO CR and VSC CR, Czech Republic; DNRF, DNSRC and Lundbeck Foundation, Denmark; EPLANET and ERC, European Union; IN2P3-CNRS, CEA-DSM/IRFU, France; GNAS, Georgia; BMBF, DFG, HGF, MPG and AvH Foundation, Germany; GSRT, Greece; ISF, MINERVA, GIF, DIP and Benozzi Center, Israel; INFN, Italy; MEXT and JSPS, Japan; CNRST, Morocco; FOM and NWO, Netherlands; RCN, Norway; MNiSW, Poland; GRICES and FCT, Portugal; MERYS (MECTS), Romania; MES of Russia and ROSATOM, Russian Federation; JINR; MSTB, Serbia; MSSR, Slovakia; ARRS and MVZT, Slovenia; DST/NRF, South Africa; MICINN, Spain; SRC and Wallenberg Foundation, Sweden; SER, SNSF and Cantons of Bern and Geneva, Switzerland; NSC, Taiwan; TAEK, Turkey; STFC, the Royal Society and Leverhulme Trust, United Kingdom; DOE and NSF, United States of America.

The crucial computing support from all WLCG partners is acknowledged gratefully, in particular from CERN and the ATLAS Tier-1 facilities at TRIUMF (Canada), NDGF (Denmark, Norway, Sweden), CC-IN2P3 (France), KIT/GridKA (Germany), INFN-CNAF (Italy), NL-T1 (Netherlands), PIC (Spain), ASGC (Taiwan), RAL (UK) and BNL (USA) and in the Tier-2 facilities worldwide.

Open access

This article is published Open Access at sciencedirect.com. It is distributed under the terms of the Creative Commons Attribution License 3.0, which permits unrestricted use, distribution, and reproduction in any medium, provided the original authors and source are credited.

References

- [1] ATLAS Collaboration, Phys. Lett. B 711 (2012) 244.
- [2] ATLAS Collaboration, JHEP 1205 (2012) 059.
- [3] CMS Collaboration, Phys. Rev. D 84 (2011) 092004.
- [4] CMS Collaboration, Eur. Phys. J. C 71 (2011) 1721.
- [5] CMS Collaboration, JHEP 1107 (2011) 1721.
- [6] DØ Collaboration, Phys. Rev. D 80 (2009), 071102(R).
- [7] CMS Collaboration, Phys. Rev. D 85 (2012) 112007.
- [8] G.L. Kane, C. Kolda, L. Roszkowski, J.D. Wells, Phys. Rev. D 49 (1994) 6173.
- [9] T. Han, M.B. Magro, Phys. Lett. B 476 (2000) 79.
- [10] C. Yue, H. Zong, L. Liu, Mod. Phys. Lett. A 18 (2003) 2187.
- [11] DØ Collaboration, Phys. Lett. B 682 (2009) 278.
- [12] ATLAS Collaboration, JHEP 1206 (2012) 039.
- [13] CMS Collaboration, JHEP 1207 (2012) 143.
- [14] ATLAS Collaboration, Performance of the reconstruction and identification of hadronic tau decays with the ATLAS detector, ATLAS-CONF-2011-152.
- [15] Y. Freund, R.E. Schapire, in: L. Saitta (Ed.), Machine Learning: Proceedings of the Thirteenth International Conference, Morgan Kaufmann, San Francisco, 1996, p. 148.
- [16] B.P. Roe, H.-J. Yang, J. Zhu, Y. Liu, I. Stancu, G. McGregor, Nucl. Instrum. Meth. A 543 (2005) 577.

- [17] ATLAS Collaboration, JINST 3 (2008) S08003.
 [18] GEANT4 Collaboration, S. Agostinelli, et al., Nucl. Instrum. Meth. A 506 (2003) 250.
 [19] ATLAS Collaboration, Eur. Phys. J. C 70 (2010) 823.
 [20] S. Frixione, B.R. Webber, JHEP 0206 (2002) 029.
 [21] S. Frixione, P. Nason, B.R. Webber, JHEP 0308 (2003) 007.
 [22] S. Frixione, E. Laenen, P. Motylinski, JHEP 0603 (2006) 092.
 [23] P.M. Nadolsky, et al., Phys. Rev. D 78 (2008) 013004.
 [24] G. Corcella, et al., JHEP 0101 (2001) 010;
 G. Corcella, et al., HERWIG 6.5 release notes, arXiv:hep-ph/0210213.
 [25] M. Aliev, et al., Comput. Phys. Commun. 182 (2011) 1034.
 [26] M.L. Mangano, M. Moretti, H. Lai, P. Nadolsky, A.D. Polosa, JHEP 0307 (2003) 001.
 [27] J. Alwall, et al., Eur. Phys. J. C 53 (2008) 473.
 [28] J. Butterworth, J.R. Forshaw, M.H. Seymour, Z. Phys. C 72 (1996) 637.
 [29] N. Davidson, et al., Universal interface of TAUOLA technical and physics documentation, arXiv:1002.0543.
 [30] ATLAS Collaboration, ATLAS tunes of PYTHIA 6 and PYTHIA 8 for MC11, ATLAS-PUB-2011-009.
 [31] M. Cacciari, G.P. Salam, G. Soyez, JHEP 0804 (2008) 063.
 [32] ATLAS Collaboration, Jet energy measurement with the ATLAS detector in proton–proton collisions at $\sqrt{s} = 7$ TeV, arXiv:1112.6426.
 [33] ATLAS Collaboration, Commissioning of the ATLAS high-performance b -tagging algorithms in the $\sqrt{s} = 7$ TeV collision data, ATLAS-CONF-2011-102.
 [34] ATLAS Collaboration, Eur. Phys. J. C 72 (2012) 1909.
 [35] ATLAS Collaboration, Muon reconstruction efficiency in reprocessed 2010 LHC proton–proton collision data recorded with the ATLAS Detector, ATLAS-CONF-2011-063.
 [36] P. Nason, JHEP 0711 (2007) 070.
 [37] S. Frixione, P. Nason, C. Oleari, JHEP 0711 (2007) 040.
 [38] S. Alioli, P. Nason, C. Oleari, E. Re, JHEP 1006 (2010) 043.
 [39] B.P. Kersevan, E. Richter-Was, The Monte Carlo event generator AcerMC version 2.0 with interfaces to PYTHIA 6.2 and HERWIG 6.5, arXiv:hep-ph/0405247.
 [40] T. Seltzer, W. Long, Comput. Phys. Commun. 81 (1994) 357.
 [41] J. Pumpli, D. Stump, J. Huston, H. Lai, P. Nadolsky, W. Tung, JHEP 0207 (2002) 012.
 [42] A.D. Martin, R.G. Roberts, W.J. Stirling, R.S. Thorne, Eur. Phys. J. C 4 (1998) 463; A.D. Martin, R.G. Roberts, W.J. Stirling, R.S. Thorne, Eur. Phys. J. C 14 (2000) 133.
 [43] CTEQ Collaboration, H. Lai, et al., Eur. Phys. J. C 12 (2000) 375.
 [44] ATLAS Collaboration, Phys. Rev. D 85 (2012) 041805.
 [45] ATLAS Collaboration, Luminosity determination in pp collisions at $\sqrt{s} = 7$ TeV using the ATLAS Detector in 2011, ATLAS-CONF-2011-016 (2011).
 [46] L. Lyons, D. Gibaut, P. Clifford, Nucl. Instrum. Meth. A 270 (1988) 110.

ATLAS Collaboration

G. Aad⁴⁸, B. Abbott¹¹¹, J. Abdallah¹¹, S. Abdel Khalek¹¹⁵, A.A. Abdelalim⁴⁹, O. Abdinov¹⁰, B. Abi¹¹², M. Abolins⁸⁸, O.S. AbouZeid¹⁵⁸, H. Abramowicz¹⁵³, H. Abreu¹³⁶, E. Acerbi^{89a,89b}, B.S. Acharya^{164a,164b}, L. Adamczyk³⁷, D.L. Adams²⁴, T.N. Addy⁵⁶, J. Adelman¹⁷⁶, S. Adomeit⁹⁸, P. Adragna⁷⁵, T. Adye¹²⁹, S. Aefsky²², J.A. Aguilar-Saavedra^{124b,a}, M. Aharrouché⁸¹, S.P. Ahlen²¹, F. Ahles⁴⁸, A. Ahmad¹⁴⁸, M. Ahsan⁴⁰, G. Aielli^{133a,133b}, T. Akdogan^{18a}, T.P.A. Åkesson⁷⁹, G. Akimoto¹⁵⁵, A.V. Akimov⁹⁴, A. Akiyama⁶⁶, M.S. Alam¹, M.A. Alam⁷⁶, J. Albert¹⁶⁹, S. Albrand⁵⁵, M. Aleksa²⁹, I.N. Aleksandrov⁶⁴, F. Alessandria^{89a}, C. Alexa^{25a}, G. Alexander¹⁵³, G. Alexandre⁴⁹, T. Alexopoulos⁹, M. Alhroob^{164a,164c}, M. Aliev¹⁵, G. Alimonti^{89a}, J. Alison¹²⁰, B.M.M. Allbrooke¹⁷, P.P. Allport⁷³, S.E. Allwood-Spiers⁵³, J. Almond⁸², A. Aloisio^{102a,102b}, R. Alon¹⁷², A. Alonso⁷⁹, B. Alvarez Gonzalez⁸⁸, M.G. Alviggi^{102a,102b}, K. Amako⁶⁵, C. Amelung²², V.V. Ammosov¹²⁸, A. Amorim^{124a,b}, G. Amorós¹⁶⁷, N. Amram¹⁵³, C. Anastopoulos²⁹, L.S. Ancu¹⁶, N. Andari¹¹⁵, T. Andeen³⁴, C.F. Anders^{58b}, G. Anders^{58a}, K.J. Anderson³⁰, A. Andreazza^{89a,89b}, V. Andrei^{58a}, X.S. Anduaga⁷⁰, P. Anger⁴³, A. Angerami³⁴, F. Anghinolfi²⁹, A. Anisenkov¹⁰⁷, N. Anjos^{124a}, A. Annovi⁴⁷, A. Antonaki⁸, M. Antonelli⁴⁷, A. Antonov⁹⁶, J. Antos^{144b}, F. Anulli^{132a}, S. Aoun⁸³, L. Aperio Bella⁴, R. Apolle^{118,c}, G. Arabidze⁸⁸, I. Aracena¹⁴³, Y. Arai⁶⁵, A.T.H. Arce⁴⁴, S. Arfaoui¹⁴⁸, J-F. Arguin¹⁴, E. Arik^{18a,*}, M. Arik^{18a}, A.J. Armbruster⁸⁷, O. Arnaez⁸¹, V. Arnal⁸⁰, C. Arnault¹¹⁵, A. Artamonov⁹⁵, G. Artoni^{132a,132b}, D. Arutinov²⁰, S. Asai¹⁵⁵, R. Asfandiyarov¹⁷³, S. Ask²⁷, B. Åsman^{146a,146b}, L. Asquith⁵, K. Assamagan²⁴, A. Astbury¹⁶⁹, B. Aubert⁴, E. Auge¹¹⁵, K. Augsten¹²⁷, M. Aurousseau^{145a}, G. Avolio¹⁶³, R. Avramidou⁹, D. Axen¹⁶⁸, G. Azuelos^{93,d}, Y. Azuma¹⁵⁵, M.A. Baak²⁹, G. Baccaglioni^{89a}, C. Bacci^{134a,134b}, A.M. Bach¹⁴, H. Bachacou¹³⁶, K. Bachas²⁹, M. Backes⁴⁹, M. Backhaus²⁰, E. Badescu^{25a}, P. Bagnaia^{132a,132b}, S. Bahinipati², Y. Bai^{32a}, D.C. Bailey¹⁵⁸, T. Bain¹⁵⁸, J.T. Baines¹²⁹, O.K. Baker¹⁷⁶, M.D. Baker²⁴, S. Baker⁷⁷, E. Banas³⁸, P. Banerjee⁹³, Sw. Banerjee¹⁷³, D. Banfi²⁹, A. Bangert¹⁵⁰, V. Bansal¹⁶⁹, H.S. Bansil¹⁷, L. Barak¹⁷², S.P. Baranov⁹⁴, A. Barbaro Galtieri¹⁴, T. Barber⁴⁸, E.L. Barberio⁸⁶, D. Barberis^{50a,50b}, M. Barbero²⁰, D.Y. Bardin⁶⁴, T. Barillari⁹⁹, M. Barisonzi¹⁷⁵, T. Barklow¹⁴³, N. Barlow²⁷, B.M. Barnett¹²⁹, R.M. Barnett¹⁴, A. Baroncelli^{134a}, G. Barone⁴⁹, A.J. Barr¹¹⁸, F. Barreiro⁸⁰, J. Barreiro Guimarães da Costa⁵⁷, P. Barrillon¹¹⁵, R. Bartoldus¹⁴³, A.E. Barton⁷¹, V. Bartsch¹⁴⁹, R.L. Bates⁵³, L. Batkova^{144a}, J.R. Batley²⁷, A. Battaglia¹⁶, M. Battistin²⁹, F. Bauer¹³⁶, H.S. Bawa^{143,e}, S. Beale⁹⁸, T. Beau⁷⁸, P.H. Beauchemin¹⁶¹, R. Beccherle^{50a}, P. Bechtel²⁰, H.P. Beck¹⁶, A.K. Becker¹⁷⁵, S. Becker⁹⁸, M. Beckingham¹³⁸, K.H. Becks¹⁷⁵, A.J. Beddall^{18c}, A. Beddall^{18c}, S. Bedikian¹⁷⁶, V.A. Bednyakov⁶⁴, C.P. Bee⁸³, M. Begel²⁴, S. Behar Harpaz¹⁵², P.K. Behera⁶², M. Beimforde⁹⁹, C. Belanger-Champagne⁸⁵, P.J. Bell⁴⁹, W.H. Bell⁴⁹, G. Bella¹⁵³, L. Bellagamba^{19a}, F. Bellina²⁹, M. Bellomo²⁹, A. Belloni⁵⁷, O. Beloborodova^{107,f}, K. Belotskiy⁹⁶, O. Beltramello²⁹, O. Benary¹⁵³, D. Bencheikroun^{135a}, K. Bendtz^{146a,146b}, N. Benekos¹⁶⁵, Y. Benhammou¹⁵³, E. Benhar Noccioli⁴⁹, J.A. Benitez Garcia^{159b}, D.P. Benjamin⁴⁴, M. Benoit¹¹⁵, J.R. Bensinger²², K. Benslama¹³⁰, S. Bentvelsen¹⁰⁵, D. Berge²⁹, E. Bergeaas Kuutmann⁴¹, N. Berger⁴, F. Berghaus¹⁶⁹, E. Berglund¹⁰⁵,

J. Beringer¹⁴, P. Bernat⁷⁷, R. Bernhard⁴⁸, C. Bernius²⁴, T. Berry⁷⁶, C. Bertella⁸³, A. Bertin^{19a,19b}, F. Bertolucci^{122a,122b}, M.I. Besana^{89a,89b}, N. Besson¹³⁶, S. Bethke⁹⁹, W. Bhimji⁴⁵, R.M. Bianchi²⁹, M. Bianco^{72a,72b}, O. Biebel⁹⁸, S.P. Bieniek⁷⁷, K. Bierwagen⁵⁴, J. Biesiada¹⁴, M. Biglietti^{134a}, H. Bilokon⁴⁷, M. Bindi^{19a,19b}, S. Binet¹¹⁵, A. Bingul^{18c}, C. Bini^{132a,132b}, C. Biscarat¹⁷⁸, U. Bitenc⁴⁸, K.M. Black²¹, R.E. Blair⁵, J.-B. Blanchard¹³⁶, G. Blanchot²⁹, T. Blazek^{144a}, C. Blocker²², J. Blocki³⁸, A. Blondel⁴⁹, W. Blum⁸¹, U. Blumenschein⁵⁴, G.J. Bobbink¹⁰⁵, V.B. Bobrovnikov¹⁰⁷, S.S. Bocchetta⁷⁹, A. Bocci⁴⁴, C.R. Boddy¹¹⁸, M. Boehler⁴¹, J. Boek¹⁷⁵, N. Boelaert³⁵, J.A. Bogaerts²⁹, A. Bogdanchikov¹⁰⁷, A. Bogouch^{90,*}, C. Bohm^{146a}, J. Bohm¹²⁵, V. Boisvert⁷⁶, T. Bold³⁷, V. Boldea^{25a}, N.M. Bolnet¹³⁶, M. Bomben⁷⁸, M. Bona⁷⁵, M. Bondioli¹⁶³, M. Boonekamp¹³⁶, C.N. Booth¹³⁹, S. Bordini⁷⁸, C. Borer¹⁶, A. Borisov¹²⁸, G. Borissov⁷¹, I. Borjanovic^{12a}, M. Borri⁸², S. Borroni⁸⁷, V. Bortolotto^{134a,134b}, K. Bos¹⁰⁵, D. Boscherini^{19a}, M. Bosman¹¹, H. Boterenbrood¹⁰⁵, D. Botterill¹²⁹, J. Bouchami⁹³, J. Boudreau¹²³, E.V. Bouhova-Thacker⁷¹, D. Boumediene³³, C. Bourdarios¹¹⁵, N. Bousson⁸³, A. Boveia³⁰, J. Boyd²⁹, I.R. Boyko⁶⁴, N.I. Bozhko¹²⁸, I. Bozovic-Jelisavcic^{12b}, J. Bracnik¹⁷, P. Branchini^{134a}, A. Brandt⁷, G. Brandt¹¹⁸, O. Brandt⁵⁴, U. Bratzler¹⁵⁶, B. Brau⁸⁴, J.E. Brau¹¹⁴, H.M. Braun¹⁷⁵, B. Brelier¹⁵⁸, J. Bremer²⁹, K. Brendlinger¹²⁰, R. Brenner¹⁶⁶, S. Bressler¹⁷², D. Britton⁵³, F.M. Brochu²⁷, I. Brock²⁰, R. Brock⁸⁸, E. Brodet¹⁵³, F. Broggi^{89a}, C. Bromberg⁸⁸, J. Bronner⁹⁹, G. Brooijmans³⁴, W.K. Brooks^{31b}, G. Brown⁸², H. Brown⁷, P.A. Bruckman de Renstrom³⁸, D. Bruncko^{144b}, R. Bruneliere⁴⁸, S. Brunet⁶⁰, A. Bruni^{19a}, G. Bruni^{19a}, M. Bruschi^{19a}, T. Buanes¹³, Q. Buat⁵⁵, F. Bucci⁴⁹, J. Buchanan¹¹⁸, P. Buchholz¹⁴¹, R.M. Buckingham¹¹⁸, A.G. Buckley⁴⁵, S.I. Buda^{25a}, I.A. Budagov⁶⁴, B. Budick¹⁰⁸, V. Büscher⁸¹, L. Bugge¹¹⁷, O. Bulekov⁹⁶, A.C. Bundock⁷³, M. Bunse⁴², T. Buran¹¹⁷, H. Burckhart²⁹, S. Burdin⁷³, T. Burgess¹³, S. Burke¹²⁹, E. Busato³³, P. Bussey⁵³, C.P. Buszello¹⁶⁶, B. Butler¹⁴³, J.M. Butler²¹, C.M. Buttar⁵³, J.M. Butterworth⁷⁷, W. Buttinger²⁷, S. Cabrera Urbán¹⁶⁷, D. Caforio^{19a,19b}, O. Cakir^{3a}, P. Calafiura¹⁴, G. Calderini⁷⁸, P. Calfayan⁹⁸, R. Calkins¹⁰⁶, L.P. Caloba^{23a}, R. Caloi^{132a,132b}, D. Calvet³³, S. Calvet³³, R. Camacho Toro³³, P. Camarri^{133a,133b}, D. Cameron¹¹⁷, L.M. Caminada¹⁴, S. Campana²⁹, M. Campanelli⁷⁷, V. Canale^{102a,102b}, F. Canelli^{30,g}, A. Canepa^{159a}, J. Cantero⁸⁰, R. Cantrill⁷⁶, L. Capasso^{102a,102b}, M.D.M. Capeans Garrido²⁹, I. Caprini^{25a}, M. Caprini^{25a}, D. Capriotti⁹⁹, M. Capua^{36a,36b}, R. Caputo⁸¹, R. Cardarelli^{133a}, T. Carli²⁹, G. Carlino^{102a}, L. Carminati^{89a,89b}, B. Caron⁸⁵, S. Caron¹⁰⁴, E. Carquin^{31b}, G.D. Carrillo Montoya¹⁷³, A.A. Carter⁷⁵, J.R. Carter²⁷, J. Carvalho^{124a,h}, D. Casadei¹⁰⁸, M.P. Casado¹¹, M. Cascella^{122a,122b}, C. Caso^{50a,50b,*}, A.M. Castaneda Hernandez¹⁷³, E. Castaneda-Miranda¹⁷³, V. Castillo Gimenez¹⁶⁷, N.F. Castro^{124a}, G. Cataldi^{72a}, P. Catastini⁵⁷, A. Catinaccio²⁹, J.R. Catmore²⁹, A. Cattai²⁹, G. Cattani^{133a,133b}, S. Caughron⁸⁸, D. Cauz^{164a,164c}, P. Cavalleri⁷⁸, D. Cavalli^{89a}, M. Cavalli-Sforza¹¹, V. Cavasinni^{122a,122b}, F. Ceradini^{134a,134b}, A.S. Cerqueira^{23b}, A. Cerri²⁹, L. Cerrito⁷⁵, F. Cerutti⁴⁷, S.A. Cetin^{18b}, A. Chafaq^{135a}, D. Chakraborty¹⁰⁶, I. Chalupkova¹²⁶, K. Chan², B. Chapleau⁸⁵, J.D. Chapman²⁷, J.W. Chapman⁸⁷, E. Chareyre⁷⁸, D.G. Charlton¹⁷, V. Chavda⁸², C.A. Chavez Barajas²⁹, S. Cheatham⁸⁵, S. Chekanov⁵, S.V. Chekulaev^{159a}, G.A. Chelkov⁶⁴, M.A. Chelstowska¹⁰⁴, C. Chen⁶³, H. Chen²⁴, S. Chen^{32c}, X. Chen¹⁷³, A. Cheplakov⁶⁴, R. Cherkaoui El Moursli^{135e}, V. Chernyatin²⁴, E. Cheu⁶, S.L. Cheung¹⁵⁸, L. Chevalier¹³⁶, G. Chiefari^{102a,102b}, L. Chikovani^{51a}, J.T. Childers²⁹, A. Chilingarov⁷¹, G. Chiodini^{72a}, A.S. Chisholm¹⁷, R.T. Chislett⁷⁷, M.V. Chizhov⁶⁴, G. Choudalakis³⁰, S. Chouridou¹³⁷, I.A. Christidi⁷⁷, A. Christov⁴⁸, D. Chromek-Burckhart²⁹, M.L. Chu¹⁵¹, J. Chudoba¹²⁵, G. Ciapetti^{132a,132b}, A.K. Ciftci^{3a}, R. Ciftci^{3a}, D. Cinca³³, V. Cindro⁷⁴, C. Ciocca^{19a,19b}, A. Ciochio¹⁴, M. Cirilli⁸⁷, M. Citterio^{89a}, M. Ciubancan^{25a}, A. Clark⁴⁹, P.J. Clark⁴⁵, W. Cleland¹²³, J.C. Clemens⁸³, B. Clement⁵⁵, C. Clement^{146a,146b}, Y. Coadou⁸³, M. Cobal^{164a,164c}, A. Coccaro¹³⁸, J. Cochran⁶³, P. Coe¹¹⁸, J.G. Cogan¹⁴³, J. Coggeshall¹⁶⁵, E. Cogneras¹⁷⁸, J. Colas⁴, A.P. Colijn¹⁰⁵, N.J. Collins¹⁷, C. Collins-Tooth⁵³, J. Collot⁵⁵, T. Colombo^{119a,119b}, G. Colon⁸⁴, P. Conde Muiño^{124a}, E. Coniavitis¹¹⁸, M.C. Conidi¹¹, S.M. Consonni^{89a,89b}, V. Consorti⁴⁸, S. Constantinescu^{25a}, C. Conta^{119a,119b}, G. Conti⁵⁷, F. Conventi^{102a,i}, M. Cooke¹⁴, B.D. Cooper⁷⁷, A.M. Cooper-Sarkar¹¹⁸, K. Copic¹⁴, T. Cornelissen¹⁷⁵, M. Corradi^{19a}, F. Corriveau^{85,j}, A. Cortes-Gonzalez¹⁶⁵, G. Cortiana⁹⁹, G. Costa^{89a}, M.J. Costa¹⁶⁷, D. Costanzo¹³⁹, T. Costin³⁰, D. Côté²⁹, L. Courneyea¹⁶⁹, G. Cowan⁷⁶, C. Cowden²⁷, B.E. Cox⁸², K. Cranmer¹⁰⁸, F. Crescioli^{122a,122b}, M. Cristinziani²⁰, G. Crosetti^{36a,36b}, R. Crupi^{72a,72b}, S. Crépe-Renaudin⁵⁵, C.-M. Cuciuc^{25a}, C. Cuenca Almenar¹⁷⁶, T. Cuhadar Donszelmann¹³⁹, M. Curatolo⁴⁷, C.J. Curtis¹⁷, C. Cuthbert¹⁵⁰, P. Cwetanski⁶⁰, H. Czirr¹⁴¹, P. Czodrowski⁴³, Z. Czynzula¹⁷⁶, S. D'Auria⁵³, M. D'Onofrio⁷³, A. D'Orazio^{132a,132b},

C. Da Via⁸², W. Dabrowski³⁷, A. Dafinca¹¹⁸, T. Dai⁸⁷, C. Dallapiccola⁸⁴, M. Dam³⁵, M. Dameri^{50a,50b}, D.S. Damiani¹³⁷, H.O. Danielsson²⁹, V. Dao⁴⁹, G. Darbo^{50a}, G.L. Darlea^{25b}, W. Davey²⁰, T. Davidek¹²⁶, N. Davidson⁸⁶, R. Davidson⁷¹, E. Davies^{118,c}, M. Davies⁹³, A.R. Davison⁷⁷, Y. Davygora^{58a}, E. Dawe¹⁴², I. Dawson¹³⁹, R.K. Daya-Ishmukhametova²², K. De⁷, R. de Asmundis^{102a}, S. De Castro^{19a,19b}, S. De Cecco⁷⁸, J. de Graat⁹⁸, N. De Groot¹⁰⁴, P. de Jong¹⁰⁵, C. De La Taille¹¹⁵, H. De la Torre⁸⁰, F. De Lorenzi⁶³, B. De Lotto^{164a,164c}, L. de Mora⁷¹, L. De Nooij¹⁰⁵, D. De Pedis^{132a}, A. De Salvo^{132a}, U. De Sanctis^{164a,164c}, A. De Santo¹⁴⁹, J.B. De Vivie De Regie¹¹⁵, G. De Zorzi^{132a,132b}, W.J. Dearnaley⁷¹, R. Debbe²⁴, C. Debenedetti⁴⁵, B. Dechenaux⁵⁵, D.V. Dedovich⁶⁴, J. Degenhardt¹²⁰, C. Del Papa^{164a,164c}, J. Del Peso⁸⁰, T. Del Prete^{122a,122b}, T. Delemontex⁵⁵, M. Deliyergiyev⁷⁴, A. Dell'Acqua²⁹, L. Dell'Asta²¹, M. Della Pietra^{102a,i}, D. della Volpe^{102a,102b}, M. Delmastro⁴, P.A. Delsart⁵⁵, C. Deluca¹⁰⁵, S. Demers¹⁷⁶, M. Demichev⁶⁴, B. Demirkoz^{11,k}, J. Deng¹⁶³, S.P. Denisov¹²⁸, D. Derendarz³⁸, J.E. Derkaoui^{135d}, F. Derue⁷⁸, P. Dervan⁷³, K. Desch²⁰, E. Devetak¹⁴⁸, P.O. Deviveiros¹⁰⁵, A. Dewhurst¹²⁹, B. DeWilde¹⁴⁸, S. Dhaliwal¹⁵⁸, R. Dhullipudi^{24,l}, A. Di Ciaccio^{133a,133b}, L. Di Ciaccio⁴, A. Di Girolamo²⁹, B. Di Girolamo²⁹, S. Di Luise^{134a,134b}, A. Di Mattia¹⁷³, B. Di Micco²⁹, R. Di Nardo⁴⁷, A. Di Simone^{133a,133b}, R. Di Sipio^{19a,19b}, M.A. Diaz^{31a}, E.B. Diehl⁸⁷, J. Dietrich⁴¹, T.A. Dietzsch^{58a}, S. Diglio⁸⁶, K. Dindar Yagci³⁹, J. Dingfelder²⁰, C. Dionisi^{132a,132b}, P. Dita^{25a}, S. Dita^{25a}, F. Dittus²⁹, F. Djama⁸³, T. Djobava^{51b}, M.A.B. do Vale^{23c}, A. Do Valle Wemans^{124a}, T.K.O. Doan⁴, M. Dobbs⁸⁵, R. Dobinson^{29,*}, D. Dobos²⁹, E. Dobson^{29,m}, J. Dodd³⁴, C. Doglioni⁴⁹, T. Doherty⁵³, Y. Doi^{65,*}, J. Dolejsi¹²⁶, I. Dolenc⁷⁴, Z. Dolezal¹²⁶, B.A. Dolgoshein^{96,*}, T. Dohmae¹⁵⁵, M. Donadelli^{23d}, M. Donega¹²⁰, J. Donini³³, J. Dopke²⁹, A. Doria^{102a}, A. Dos Anjos¹⁷³, A. Dotti^{122a,122b}, M.T. Dova⁷⁰, A.D. Doxiadis¹⁰⁵, A.T. Doyle⁵³, M. Dris⁹, J. Dubbert⁹⁹, S. Dube¹⁴, E. Duchovni¹⁷², G. Duckeck⁹⁸, A. Dudarev²⁹, F. Dudziak⁶³, M. Dührssen²⁹, I.P. Duerdoth⁸², L. Dufлот¹¹⁵, M-A. Dufour⁸⁵, M. Dunford²⁹, H. Duran Yildiz^{3a}, R. Duxfield¹³⁹, M. Dwuznik³⁷, F. Dydak²⁹, M. Düren⁵², J. Ebke⁹⁸, S. Eckweiler⁸¹, K. Edmonds⁸¹, C.A. Edwards⁷⁶, N.C. Edwards⁵³, W. Ehrenfeld⁴¹, T. Eifert¹⁴³, G. Eigen¹³, K. Einsweiler¹⁴, E. Eisenhandler⁷⁵, T. Ekelof¹⁶⁶, M. El Kacimi^{135c}, M. Ellert¹⁶⁶, S. Elles⁴, F. Ellinghaus⁸¹, K. Ellis⁷⁵, N. Ellis²⁹, J. Elmsheuser⁹⁸, M. Elsing²⁹, D. Emeliyanov¹²⁹, R. Engelmann¹⁴⁸, A. Engl⁹⁸, B. Epp⁶¹, A. Eppig⁸⁷, J. Erdmann⁵⁴, A. Ereditato¹⁶, D. Eriksson^{146a}, J. Ernst¹, M. Ernst²⁴, J. Ernwein¹³⁶, D. Errede¹⁶⁵, S. Errede¹⁶⁵, E. Ertel⁸¹, M. Escalier¹¹⁵, C. Escobar¹²³, X. Espinal Curull¹¹, B. Esposito⁴⁷, F. Etienne⁸³, A.I. Etievre¹³⁶, E. Etzion¹⁵³, D. Evangelakou⁵⁴, H. Evans⁶⁰, L. Fabbri^{19a,19b}, C. Fabre²⁹, R.M. Fakhruddinov¹²⁸, S. Falciano^{132a}, Y. Fang¹⁷³, M. Fanti^{89a,89b}, A. Farbin⁷, A. Farilla^{134a}, J. Farley¹⁴⁸, T. Farooque¹⁵⁸, S. Farrell¹⁶³, S.M. Farrington¹¹⁸, P. Farthouat²⁹, P. Fassnacht²⁹, D. Fassouliotis⁸, B. Fatholahzadeh¹⁵⁸, A. Favareto^{89a,89b}, L. Fayard¹¹⁵, S. Fazio^{36a,36b}, R. Febbraro³³, P. Federic^{144a}, O.L. Fedin¹²¹, W. Fedorko⁸⁸, M. Fehling-Kaschek⁴⁸, L. Feligioni⁸³, D. Fellmann⁵, C. Feng^{32d}, E.J. Feng³⁰, A.B. Fenyuk¹²⁸, J. Ferencei^{144b}, W. Fernando⁵, S. Ferrag⁵³, J. Ferrando⁵³, V. Ferrara⁴¹, A. Ferrari¹⁶⁶, P. Ferrari¹⁰⁵, R. Ferrari^{119a}, D.E. Ferreira de Lima⁵³, A. Ferrer¹⁶⁷, D. Ferrere⁴⁹, C. Ferretti⁸⁷, A. Ferretto Parodi^{50a,50b}, M. Fiascaris³⁰, F. Fiedler⁸¹, A. Filipčič⁷⁴, F. Filthaut¹⁰⁴, M. Fincke-Keeler¹⁶⁹, M.C.N. Fiolhais^{124a,h}, L. Fiorini¹⁶⁷, A. Firan³⁹, G. Fischer⁴¹, M.J. Fisher¹⁰⁹, M. Flechl⁴⁸, I. Fleck¹⁴¹, J. Fleckner⁸¹, P. Fleischmann¹⁷⁴, S. Fleischmann¹⁷⁵, T. Flick¹⁷⁵, A. Floderus⁷⁹, L.R. Flores Castillo¹⁷³, M.J. Flowerdew⁹⁹, T. Fonseca Martin¹⁶, D.A. Forbush¹³⁸, A. Formica¹³⁶, A. Forti⁸², D. Fortin^{159a}, D. Fournier¹¹⁵, H. Fox⁷¹, P. Francavilla¹¹, S. Franchino^{119a,119b}, D. Francis²⁹, T. Frank¹⁷², M. Franklin⁵⁷, S. Franz²⁹, M. Fraternali^{119a,119b}, S. Fratina¹²⁰, S.T. French²⁷, C. Friedrich⁴¹, F. Friedrich⁴³, R. Froeschl²⁹, D. Froidevaux²⁹, J.A. Frost²⁷, C. Fukunaga¹⁵⁶, E. Fullana Torregrosa²⁹, B.G. Fulsom¹⁴³, J. Fuster¹⁶⁷, C. Gabaldon²⁹, O. Gabizon¹⁷², T. Gadfort²⁴, S. Gadomski⁴⁹, G. Gagliardi^{50a,50b}, P. Gagnon⁶⁰, C. Galea⁹⁸, E.J. Gallas¹¹⁸, V. Gallo¹⁶, B.J. Gallop¹²⁹, P. Gallus¹²⁵, K.K. Gan¹⁰⁹, Y.S. Gao^{143,e}, A. Gaponenko¹⁴, F. Garberon¹⁷⁶, M. Garcia-Sciveres¹⁴, C. García¹⁶⁷, J.E. García Navarro¹⁶⁷, R.W. Gardner³⁰, N. Garelli²⁹, H. Garitaonandia¹⁰⁵, V. Garonne²⁹, J. Garvey¹⁷, C. Gatti⁴⁷, G. Gaudio^{119a}, B. Gaur¹⁴¹, L. Gauthier¹³⁶, P. Gauzzi^{132a,132b}, I.L. Gavrilenko⁹⁴, C. Gay¹⁶⁸, G. Gaycken²⁰, E.N. Gazis⁹, P. Ge^{32d}, Z. Gece¹⁶⁸, C.N.P. Gee¹²⁹, D.A.A. Geerts¹⁰⁵, Ch. Geich-Gimbel²⁰, K. Gellerstedt^{146a,146b}, C. Gemme^{50a}, A. Gemmell⁵³, M.H. Genest⁵⁵, S. Gentile^{132a,132b}, M. George⁵⁴, S. George⁷⁶, P. Gerlach¹⁷⁵, A. Gershon¹⁵³, C. Geweniger^{58a}, H. Ghazlane^{135b}, N. Ghodbane³³, B. Giacobbe^{19a}, S. Giagu^{132a,132b}, V. Giakoumopoulou⁸, V. Giangiobbe¹¹, F. Gianotti²⁹, B. Gibbard²⁴, A. Gibson¹⁵⁸, S.M. Gibson²⁹, D. Gillberg²⁸, A.R. Gillman¹²⁹, D.M. Gingrich^{2,d}, J. Ginzburg¹⁵³, N. Giokaris⁸, M.P. Giordani^{164c},

R. Giordano^{102a,102b}, F.M. Giorgi¹⁵, P. Giovannini⁹⁹, P.F. Giraud¹³⁶, D. Giugni^{89a}, M. Giunta⁹³, P. Giusti^{19a}, B.K. Gjelsten¹¹⁷, L.K. Gladilin⁹⁷, C. Glasman⁸⁰, J. Glatzer⁴⁸, A. Glazov⁴¹, K.W. Glitza¹⁷⁵, G.L. Glonti⁶⁴, J.R. Goddard⁷⁵, J. Godfrey¹⁴², J. Godlewski²⁹, M. Goebel⁴¹, T. Göpfert⁴³, C. Goeringer⁸¹, C. Gössling⁴², S. Goldfarb⁸⁷, T. Golling¹⁷⁶, A. Gomes^{124a,b}, L.S. Gomez Fajardo⁴¹, R. Gonçalo⁷⁶, J. Goncalves Pinto Firmino Da Costa⁴¹, L. Gonella²⁰, S. Gonzalez¹⁷³, S. González de la Hoz¹⁶⁷, G. Gonzalez Parra¹¹, M.L. Gonzalez Silva²⁶, S. Gonzalez-Sevilla⁴⁹, J.J. Goodson¹⁴⁸, L. Goossens²⁹, P.A. Gorbounov⁹⁵, H.A. Gordon²⁴, I. Gorelov¹⁰³, G. Gorfine¹⁷⁵, B. Gorini²⁹, E. Gorini^{72a,72b}, A. Gorišek⁷⁴, E. Gornicki³⁸, B. Gosdzik⁴¹, A.T. Goshaw⁵, M. Gosselink¹⁰⁵, M.I. Gostkin⁶⁴, I. Gough Eschrich¹⁶³, M. Gouighri^{135a}, D. Goujdami^{135c}, M.P. Goulette⁴⁹, A.G. Goussiou¹³⁸, C. Goy⁴, S. Gozpinar²², I. Grabowska-Bold³⁷, P. Grafström²⁹, K.-J. Grahm⁴¹, F. Grancagnolo^{72a}, S. Grancagnolo¹⁵, V. Grassi¹⁴⁸, V. Gratchev¹²¹, N. Grau³⁴, H.M. Gray²⁹, J.A. Gray¹⁴⁸, E. Graziani^{134a}, O.G. Grebenyuk¹²¹, T. Greenshaw⁷³, Z.D. Greenwood^{24,l}, K. Gregersen³⁵, I.M. Gregor⁴¹, P. Grenier¹⁴³, J. Griffiths¹³⁸, N. Grigalashvili⁶⁴, A.A. Grillo¹³⁷, S. Grinstein¹¹, Y.V. Grishkevich⁹⁷, J.-F. Grivaz¹¹⁵, E. Gross¹⁷², J. Grosse-Knetter⁵⁴, J. Groth-Jensen¹⁷², K. Grybel¹⁴¹, D. Guest¹⁷⁶, C. Guicheney³³, A. Guida^{72a,72b}, S. Guindon⁵⁴, H. Guler^{85,n}, J. Gunther¹²⁵, B. Guo¹⁵⁸, J. Guo³⁴, V.N. Gushchin¹²⁸, P. Gutierrez¹¹¹, N. Guttman¹⁵³, O. Gutzwiller¹⁷³, C. Guyot¹³⁶, C. Gwenlan¹¹⁸, C.B. Gwilliam⁷³, A. Haas¹⁴³, S. Haas²⁹, C. Haber¹⁴, H.K. Hadavand³⁹, D.R. Hadley¹⁷, P. Haefner⁹⁹, F. Hahn²⁹, S. Haider²⁹, Z. Hajduk³⁸, H. Hakobyan¹⁷⁷, D. Hall¹¹⁸, J. Haller⁵⁴, K. Hamacher¹⁷⁵, P. Hamal¹¹³, M. Hamer⁵⁴, A. Hamilton^{145b,o}, S. Hamilton¹⁶¹, L. Han^{32b}, K. Hanagaki¹¹⁶, K. Hanawa¹⁶⁰, M. Hance¹⁴, C. Handel⁸¹, P. Hanke^{58a}, J.R. Hansen³⁵, J.B. Hansen³⁵, J.D. Hansen³⁵, P.H. Hansen³⁵, P. Hansson¹⁴³, K. Hara¹⁶⁰, G.A. Hare¹³⁷, T. Harenberg¹⁷⁵, S. Harkusha⁹⁰, D. Harper⁸⁷, R.D. Harrington⁴⁵, O.M. Harris¹³⁸, K. Harrison¹⁷, J. Hartert⁴⁸, F. Hartjes¹⁰⁵, T. Haruyama⁶⁵, A. Harvey⁵⁶, S. Hasegawa¹⁰¹, Y. Hasegawa¹⁴⁰, S. Hassani¹³⁶, S. Haug¹⁶, M. Hauschild²⁹, R. Hauser⁸⁸, M. Havranek²⁰, C.M. Hawkes¹⁷, R.J. Hawkins²⁹, A.D. Hawkins⁷⁹, D. Hawkins¹⁶³, T. Hayakawa⁶⁶, T. Hayashi¹⁶⁰, D. Hayden⁷⁶, C.P. Hays¹¹⁸, H.S. Hayward⁷³, S.J. Haywood¹²⁹, M. He^{32d}, S.J. Head¹⁷, V. Hedberg⁷⁹, L. Heelan⁷, S. Heim⁸⁸, B. Heinemann¹⁴, S. Heisterkamp³⁵, L. Helary⁴, C. Heller⁹⁸, M. Heller²⁹, S. Hellman^{146a,146b}, D. Hellmich²⁰, C. Hensens¹¹, R.C.W. Henderson⁷¹, M. Henke^{58a}, A. Henrichs⁵⁴, A.M. Henriques Correia²⁹, S. Henrot-Versille¹¹⁵, F. Henry-Couannier⁸³, C. Hensel⁵⁴, T. Henß¹⁷⁵, C.M. Hernandez⁷, Y. Hernández Jiménez¹⁶⁷, R. Herrberg¹⁵, G. Herten⁴⁸, R. Hertenberger⁹⁸, L. Hervas²⁹, G.G. Hesketh⁷⁷, N.P. Hessey¹⁰⁵, E. Higón-Rodríguez¹⁶⁷, J.C. Hill²⁷, K.H. Hiller⁴¹, S. Hillert²⁰, S.J. Hillier¹⁷, I. Hinchliffe¹⁴, E. Hines¹²⁰, M. Hirose¹¹⁶, F. Hirsch⁴², D. Hirschbuehl¹⁷⁵, J. Hobbs¹⁴⁸, N. Hod¹⁵³, M.C. Hodgkinson¹³⁹, P. Hodgson¹³⁹, A. Hoecker²⁹, M.R. Hoferkamp¹⁰³, J. Hoffman³⁹, D. Hoffmann⁸³, M. Hohlfeld⁸¹, M. Holder¹⁴¹, S.O. Holmgren^{146a}, T. Holy¹²⁷, J.L. Holzbauer⁸⁸, T.M. Hong¹²⁰, L. Hooft van Huysduynen¹⁰⁸, C. Horn¹⁴³, S. Horner⁴⁸, J.-Y. Hostachy⁵⁵, S. Hou¹⁵¹, A. Hoummada^{135a}, J. Howard¹¹⁸, J. Howarth⁸², I. Hristova¹⁵, J. Hrivnac¹¹⁵, I. Hruska¹²⁵, T. Hryn'ova⁴, P.J. Hsu⁸¹, S.-C. Hsu¹⁴, Z. Hubacek¹²⁷, F. Hubaut⁸³, F. Huegging²⁰, A. Huettmann⁴¹, T.B. Huffman¹¹⁸, E.W. Hughes³⁴, G. Hughes⁷¹, M. Huhtinen²⁹, M. Hurwitz¹⁴, U. Husemann⁴¹, N. Huseynov^{64,p}, J. Huston⁸⁸, J. Huth⁵⁷, G. Iacobucci⁴⁹, G. Iakovidis⁹, M. Ibbotson⁸², I. Ibragimov¹⁴¹, L. Iconomidou-Fayard¹¹⁵, J. Idarraga¹¹⁵, P. Iengo^{102a}, O. Igonkina¹⁰⁵, Y. Ikegami⁶⁵, M. Ikeno⁶⁵, D. Iliadis¹⁵⁴, N. Ilic¹⁵⁸, M. Imori¹⁵⁵, T. Ince²⁰, J. Inigo-Golfin²⁹, P. Ioannou⁸, M. Iodice^{134a}, K. Iordanidou⁸, V. Ippolito^{132a,132b}, A. Irlles Quiles¹⁶⁷, C. Isaksson¹⁶⁶, A. Ishikawa⁶⁶, M. Ishino⁶⁷, R. Ishmukhametov³⁹, C. Issever¹¹⁸, S. Istin^{18a}, A.V. Ivashin¹²⁸, W. Iwanski³⁸, H. Iwasaki⁶⁵, J.M. Izen⁴⁰, V. Izzo^{102a}, B. Jackson¹²⁰, J.N. Jackson⁷³, P. Jackson¹⁴³, M.R. Jaekel²⁹, V. Jain⁶⁰, K. Jakobs⁴⁸, S. Jakobsen³⁵, T. Jakoubek¹²⁵, J. Jakubek¹²⁷, D.K. Jana¹¹¹, E. Jansen⁷⁷, H. Jansen²⁹, A. Jantsch⁹⁹, M. Janus⁴⁸, G. Jarlskog⁷⁹, L. Jeanty⁵⁷, I. Jen-La Plante³⁰, P. Jenni²⁹, A. Jeremie⁴, P. Jež³⁵, S. Jézéquel⁴, M.K. Jha^{19a}, H. Ji¹⁷³, W. Ji⁸¹, J. Jia¹⁴⁸, Y. Jiang^{32b}, M. Jimenez Belenguer⁴¹, S. Jin^{32a}, O. Jinnouchi¹⁵⁷, M.D. Joergensen³⁵, D. Joffe³⁹, L.G. Johansen¹³, M. Johansen^{146a,146b}, K.E. Johansson^{146a}, P. Johansson¹³⁹, S. Johnert⁴¹, K.A. Johns⁶, K. Jon-And^{146a,146b}, G. Jones¹⁷⁰, R.W.L. Jones⁷¹, T.J. Jones⁷³, C. Joram²⁹, P.M. Jorge^{124a}, K.D. Joshi⁸², J. Jovicevic¹⁴⁷, T. Jovin^{12b}, X. Ju¹⁷³, C.A. Jung⁴², R.M. Jungst²⁹, V. Juranek¹²⁵, P. Jussel⁶¹, A. Juste Rozas¹¹, S. Kabana¹⁶, M. Kaci¹⁶⁷, A. Kaczmarska³⁸, P. Kadlecik³⁵, M. Kado¹¹⁵, H. Kagan¹⁰⁹, M. Kagan⁵⁷, E. Kajomovitz¹⁵², S. Kalinin¹⁷⁵, L.V. Kalinovskaya⁶⁴, S. Kama³⁹, N. Kanaya¹⁵⁵, M. Kaneda²⁹, S. Kaneti²⁷, T. Kanno¹⁵⁷, V.A. Kantserov⁹⁶, J. Kanzaki⁶⁵, B. Kaplan¹⁷⁶,

A. Kapliy³⁰, J. Kaplon²⁹, D. Kar⁵³, M. Karagounis²⁰, M. Karnevskiy⁴¹, V. Kartvelishvili⁷¹,
 A.N. Karyukhin¹²⁸, L. Kashif¹⁷³, G. Kasieczka^{58b}, R.D. Kass¹⁰⁹, A. Kastanas¹³, M. Kataoka⁴,
 Y. Kataoka¹⁵⁵, E. Katsoufis⁹, J. Katzy⁴¹, V. Kaushik⁶, K. Kawagoe⁶⁹, T. Kawamoto¹⁵⁵, G. Kawamura⁸¹,
 M.S. Kayl¹⁰⁵, V.A. Kazanin¹⁰⁷, M.Y. Kazarinov⁶⁴, R. Keeler¹⁶⁹, R. Kehoe³⁹, M. Keil⁵⁴, G.D. Kekelidze⁶⁴,
 J.S. Keller¹³⁸, J. Kennedy⁹⁸, M. Kenyon⁵³, O. Kepka¹²⁵, N. Kerschen²⁹, B.P. Kerševan⁷⁴, S. Kersten¹⁷⁵,
 K. Kessoku¹⁵⁵, J. Keung¹⁵⁸, F. Khalil-zada¹⁰, H. Khandanyan¹⁶⁵, A. Khanov¹¹², D. Kharchenko⁶⁴,
 A. Khodinov⁹⁶, A. Khomich^{58a}, T.J. Khoo²⁷, G. Khoriauli²⁰, A. Khoroshilov¹⁷⁵, V. Khovanskiy⁹⁵,
 E. Khramov⁶⁴, J. Khubua^{51b}, H. Kim^{146a,146b}, M.S. Kim², S.H. Kim¹⁶⁰, N. Kimura¹⁷¹, O. Kind¹⁵,
 B.T. King⁷³, M. King⁶⁶, R.S.B. King¹¹⁸, J. Kirk¹²⁹, A.E. Kiryunin⁹⁹, T. Kishimoto⁶⁶, D. Kisielewska³⁷,
 T. Kittelmann¹²³, A.M. Kiver¹²⁸, E. Kladiva^{144b}, M. Klein⁷³, U. Klein⁷³, K. Kleinknecht⁸¹, M. Klemetti⁸⁵,
 A. Klier¹⁷², P. Klimek^{146a,146b}, A. Klimentov²⁴, R. Klingenberg⁴², J.A. Klinger⁸², E.B. Klinkby³⁵,
 T. Klioutchnikova²⁹, P.F. Klok¹⁰⁴, S. Klous¹⁰⁵, E.-E. Kluge^{58a}, T. Kluge⁷³, P. Kluit¹⁰⁵, S. Kluth⁹⁹,
 N.S. Knecht¹⁵⁸, E. Kneringer⁶¹, E.B.F.G. Knoop⁸³, A. Knue⁵⁴, B.R. Ko⁴⁴, T. Kobayashi¹⁵⁵, M. Kobel⁴³,
 M. Kocian¹⁴³, P. Kodys¹²⁶, K. Köneke²⁹, A.C. König¹⁰⁴, S. Koenig⁸¹, L. Köpke⁸¹, F. Koetsveld¹⁰⁴,
 P. Koevesarki²⁰, T. Koffas²⁸, E. Koffeman¹⁰⁵, L.A. Kogan¹¹⁸, S. Kohlmann¹⁷⁵, F. Kohn⁵⁴, Z. Kohout¹²⁷,
 T. Kohriki⁶⁵, T. Koi¹⁴³, G.M. Kolachev¹⁰⁷, H. Kolanoski¹⁵, V. Kolesnikov⁶⁴, I. Koletsou^{89a}, J. Koll⁸⁸,
 M. Kollefrath⁴⁸, A.A. Komar⁹⁴, Y. Komori¹⁵⁵, T. Kondo⁶⁵, T. Kono^{41,q}, A.I. Kononov⁴⁸, R. Konoplich^{108,r},
 N. Konstantinidis⁷⁷, A. Kootz¹⁷⁵, S. Koperny³⁷, K. Korcyl³⁸, K. Kordas¹⁵⁴, A. Korn¹¹⁸, A. Korol¹⁰⁷,
 I. Korolkov¹¹, E.V. Korolkova¹³⁹, V.A. Korotkov¹²⁸, O. Kortner⁹⁹, S. Kortner⁹⁹, V.V. Kostyukhin²⁰,
 S. Kotov⁹⁹, V.M. Kotov⁶⁴, A. Kotwal⁴⁴, C. Kourkoumelis⁸, V. Kouskoura¹⁵⁴, A. Koutsman^{159a},
 R. Kowalewski¹⁶⁹, T.Z. Kowalski³⁷, W. Kozanecki¹³⁶, A.S. Kozhin¹²⁸, V. Kral¹²⁷, V.A. Kramarenko⁹⁷,
 G. Kramberger⁷⁴, M.W. Krasny⁷⁸, A. Krasznahorkay¹⁰⁸, J. Kraus⁸⁸, J.K. Kraus²⁰, F. Krejci¹²⁷,
 J. Kretzschmar⁷³, N. Krieger⁵⁴, P. Krieger¹⁵⁸, K. Kroeninger⁵⁴, H. Kroha⁹⁹, J. Kroll¹²⁰, J. Kroseberg²⁰,
 J. Krstic^{12a}, U. Kruchonak⁶⁴, H. Krüger²⁰, T. Kruker¹⁶, N. Krumnack⁶³, Z.V. Krumshteyn⁶⁴, A. Kruth²⁰,
 T. Kubota⁸⁶, S. Kuday^{3a}, S. Kuehn⁴⁸, A. Kugel^{58c}, T. Kuhl⁴¹, D. Kuhn⁶¹, V. Kukhtin⁶⁴, Y. Kulchitsky⁹⁰,
 S. Kuleshov^{31b}, C. Kummer⁹⁸, M. Kuna⁷⁸, J. Kunkle¹²⁰, A. Kupco¹²⁵, H. Kurashige⁶⁶, M. Kurata¹⁶⁰,
 Y.A. Kurochkin⁹⁰, V. Kus¹²⁵, E.S. Kuwertz¹⁴⁷, M. Kuze¹⁵⁷, J. Kvita¹⁴², R. Kwee¹⁵, A. La Rosa⁴⁹,
 L. La Rotonda^{36a,36b}, L. Labarga⁸⁰, J. Labbe⁴, S. Lablak^{135a}, C. Lacasta¹⁶⁷, F. Lacava^{132a,132b}, H. Lacker¹⁵,
 D. Lacour⁷⁸, V.R. Lacuesta¹⁶⁷, E. Ladygin⁶⁴, R. Lafaye⁴, B. Laforge⁷⁸, T. Lagouri⁸⁰, S. Lai⁴⁸, E. Laisne⁵⁵,
 M. Lamanna²⁹, L. Lambourne⁷⁷, C.L. Lampen⁶, W. Lampl⁶, E. Lancon¹³⁶, U. Landgraf⁴⁸, M.P.J. Landon⁷⁵,
 J.L. Lane⁸², C. Lange⁴¹, A.J. Lankford¹⁶³, F. Lanni²⁴, K. Lantzsck¹⁷⁵, S. Laplace⁷⁸, C. Lapoire²⁰,
 J.F. Laporte¹³⁶, T. Lari^{89a}, A. Larner¹¹⁸, M. Lassnig²⁹, P. Laurelli⁴⁷, V. Lavorini^{36a,36b}, W. Lavrijsen¹⁴,
 P. Laycock⁷³, O. Le Dortz⁷⁸, E. Le Guirriec⁸³, C. Le Maner¹⁵⁸, E. Le Menedeu¹¹, T. LeCompte⁵,
 F. Ledroit-Guillon⁵⁵, H. Lee¹⁰⁵, J.S.H. Lee¹¹⁶, S.C. Lee¹⁵¹, L. Lee¹⁷⁶, M. Lefebvre¹⁶⁹, M. Legendre¹³⁶,
 B.C. LeGeyt¹²⁰, F. Legger⁹⁸, C. Leggett¹⁴, M. Lehmacher²⁰, G. Lehmann Miotto²⁹, X. Lei⁶,
 M.A.L. Leite^{23d}, R. Leitner¹²⁶, D. Lellouch¹⁷², B. Lemmer⁵⁴, V. Lendermann^{58a}, K.J.C. Leney^{145b},
 T. Lenz¹⁰⁵, G. Lenzen¹⁷⁵, B. Lenzi²⁹, K. Leonhardt⁴³, S. Leontsinis⁹, F. Lepold^{58a}, C. Leroy⁹³,
 J.-R. Lessard¹⁶⁹, C.G. Lester²⁷, C.M. Lester¹²⁰, J. Levêque⁴, D. Levin⁸⁷, L.J. Levinson¹⁷², A. Lewis¹¹⁸,
 G.H. Lewis¹⁰⁸, A.M. Leyko²⁰, M. Leyton¹⁵, B. Li⁸³, H. Li^{173,s}, S. Li^{32b,t}, X. Li⁸⁷, Z. Liang^{118,u}, H. Liao³³,
 B. Liberti^{133a}, P. Lichard²⁹, M. Lichtnecker⁹⁸, K. Lie¹⁶⁵, W. Liebig¹³, C. Limbach²⁰, A. Limosani⁸⁶,
 M. Limper⁶², S.C. Lin^{151,v}, F. Linde¹⁰⁵, J.T. Linnemann⁸⁸, E. Lipeles¹²⁰, A. Lipniacka¹³, T.M. Liss¹⁶⁵,
 D. Lissauer²⁴, A. Lister⁴⁹, A.M. Litke¹³⁷, C. Liu²⁸, D. Liu¹⁵¹, H. Liu⁸⁷, J.B. Liu⁸⁷, M. Liu^{32b}, Y. Liu^{32b},
 M. Livan^{119a,119b}, S.S.A. Livermore¹¹⁸, A. Lleres⁵⁵, J. Llorente Merino⁸⁰, S.L. Lloyd⁷⁵, E. Lobodzinska⁴¹,
 P. Loch⁶, W.S. Lockman¹³⁷, T. Lodenkoetter²⁰, F.K. Loebinger⁸², A. Loginov¹⁷⁶, C.W. Loh¹⁶⁸, T. Lohse¹⁵,
 K. Lohwasser⁴⁸, M. Lokajicek¹²⁵, V.P. Lombardo⁴, R.E. Long⁷¹, L. Lopes^{124a}, D. Lopez Mateos⁵⁷,
 J. Lorenz⁹⁸, N. Lorenzo Martinez¹¹⁵, M. Losada¹⁶², P. Loscutoff¹⁴, F. Lo Sterzo^{132a,132b}, M.J. Losty^{159a},
 X. Lou⁴⁰, A. Lounis¹¹⁵, K.F. Loureiro¹⁶², J. Love²¹, P.A. Love⁷¹, A.J. Lowe^{143,e}, F. Lu^{32a}, H.J. Lubatti¹³⁸,
 C. Luci^{132a,132b}, A. Lucotte⁵⁵, A. Ludwig⁴³, D. Ludwig⁴¹, I. Ludwig⁴⁸, J. Ludwig⁴⁸, F. Luehring⁶⁰,
 G. Luijckx¹⁰⁵, W. Lukas⁶¹, D. Lumb⁴⁸, L. Luminari^{132a}, E. Lund¹¹⁷, B. Lund-Jensen¹⁴⁷, B. Lundberg⁷⁹,
 J. Lundberg^{146a,146b}, J. Lundquist³⁵, M. Lungwitz⁸¹, D. Lynn²⁴, E. Lytken⁷⁹, H. Ma²⁴, L.L. Ma¹⁷³,
 J.A. Macana Goia⁹³, G. Maccarrone⁴⁷, A. Macchiolo⁹⁹, B. Maček⁷⁴, J. Machado Miguens^{124a},
 R. Mackeprang³⁵, R.J. Madaras¹⁴, W.F. Mader⁴³, R. Maenner^{58c}, T. Maeno²⁴, P. Mättig¹⁷⁵, S. Mättig⁴¹,

L. Magnoni²⁹, E. Magradze⁵⁴, K. Mahboubi⁴⁸, S. Mahmoud⁷³, G. Mahout¹⁷, C. Maiani¹³⁶,
 C. Maidantchik^{23a}, A. Maio^{124a,b}, S. Majewski²⁴, Y. Makida⁶⁵, N. Makovec¹¹⁵, P. Mal¹³⁶, B. Malaescu²⁹,
 Pa. Malecki³⁸, P. Malecki³⁸, V.P. Maleev¹²¹, F. Malek⁵⁵, U. Mallik⁶², D. Malon⁵, C. Malone¹⁴³,
 S. Maltezos⁹, V. Malyshev¹⁰⁷, S. Malyukov²⁹, R. Mameghani⁹⁸, J. Mamuzic^{12b}, A. Manabe⁶⁵,
 L. Mandelli^{89a}, I. Mandić⁷⁴, R. Mandrysch¹⁵, J. Maneira^{124a}, P.S. Mangedard⁸⁸,
 L. Manhaes de Andrade Filho^{23a}, A. Mann⁵⁴, P.M. Manning¹³⁷, A. Manousakis-Katsikakis⁸,
 B. Mansoulie¹³⁶, A. Mapelli²⁹, L. Mapelli²⁹, L. March⁸⁰, J.F. Marchand²⁸, F. Marchese^{133a,133b},
 G. Marchiori⁷⁸, M. Marcisovsky¹²⁵, C.P. Marino¹⁶⁹, F. Marroquim^{23a}, Z. Marshall²⁹, F.K. Martens¹⁵⁸,
 S. Marti-Garcia¹⁶⁷, B. Martin²⁹, B. Martin⁸⁸, J.P. Martin⁹³, T.A. Martin¹⁷, V.J. Martin⁴⁵,
 B. Martin dit Latour⁴⁹, S. Martin-Haugh¹⁴⁹, M. Martinez¹¹, V. Martinez Outschoorn⁵⁷,
 A.C. Martyniuk¹⁶⁹, M. Marx⁸², F. Marzano^{132a}, A. Marzin¹¹¹, L. Masetti⁸¹, T. Mashimo¹⁵⁵,
 R. Mashinistov⁹⁴, J. Masik⁸², A.L. Maslennikov¹⁰⁷, I. Massa^{19a,19b}, G. Massaro¹⁰⁵, N. Massol⁴,
 A. Mastroberardino^{36a,36b}, T. Masubuchi¹⁵⁵, P. Matricon¹¹⁵, H. Matsunaga¹⁵⁵, T. Matsushita⁶⁶,
 C. Mattraversi^{118,c}, J. Maurer⁸³, S.J. Maxfield⁷³, A. Mayne¹³⁹, R. Mazini¹⁵¹, M. Mazur²⁰,
 L. Mazzaferro^{133a,133b}, M. Mazzanti^{89a}, S.P. Mc Kee⁸⁷, A. McCarn¹⁶⁵, R.L. McCarthy¹⁴⁸, T.G. McCarthy²⁸,
 N.A. McCubbin¹²⁹, K.W. McFarlane⁵⁶, J.A. McFayden¹³⁹, H. McGlone⁵³, G. Mchedlidze^{51b},
 T. McLaughlan¹⁷, S.J. McMahon¹²⁹, R.A. McPherson^{169,j}, A. Meade⁸⁴, J. Mechnich¹⁰⁵, M. Mechtel¹⁷⁵,
 M. Medinnis⁴¹, R. Meera-Lebbai¹¹¹, T. Meguro¹¹⁶, S. Mehlhase³⁵, A. Mehta⁷³, K. Meier^{58a},
 B. Meirose⁷⁹, C. Melachrinou³⁰, B.R. Mellado Garcia¹⁷³, F. Meloni^{89a,89b}, L. Mendoza Navas¹⁶²,
 Z. Meng^{151,s}, A. Mengarelli^{19a,19b}, S. Menke⁹⁹, E. Meoni¹¹, K.M. Mercurio⁵⁷, P. Mermod⁴⁹,
 L. Merola^{102a,102b}, C. Meroni^{89a}, F.S. Merritt³⁰, H. Merritt¹⁰⁹, A. Messina^{29,w}, J. Metcalfe¹⁰³,
 A.S. Mete¹⁶³, C. Meyer⁸¹, C. Meyer³⁰, J.-P. Meyer¹³⁶, J. Meyer¹⁷⁴, J. Meyer⁵⁴, T.C. Meyer²⁹,
 W.T. Meyer⁶³, J. Miao^{32d}, S. Michal²⁹, L. Micu^{25a}, R.P. Middleton¹²⁹, S. Migas⁷³, L. Mijović⁴¹,
 G. Mikenberg¹⁷², M. Mikestikova¹²⁵, M. Mikuž⁷⁴, D.W. Miller³⁰, R.J. Miller⁸⁸, W.J. Mills¹⁶⁸, C. Mills⁵⁷,
 A. Milov¹⁷², D.A. Milstead^{146a,146b}, D. Milstein¹⁷², A.A. Minaenko¹²⁸, M. Miñano Moya¹⁶⁷,
 I.A. Minashvili⁶⁴, A.I. Mincer¹⁰⁸, B. Mindur³⁷, M. Mineev⁶⁴, Y. Ming¹⁷³, L.M. Mir¹¹, G. Mirabelli^{132a},
 J. Mitrevski¹³⁷, V.A. Mitsou¹⁶⁷, S. Mitsui⁶⁵, P.S. Miyagawa¹³⁹, K. Miyazaki⁶⁶, J.U. Mjörnmark⁷⁹,
 T. Moa^{146a,146b}, P. Mockett¹³⁸, S. Moed⁵⁷, V. Moeller²⁷, K. Mönig⁴¹, N. Möser²⁰, S. Mohapatra¹⁴⁸,
 W. Mohr⁴⁸, R. Moles-Valls¹⁶⁷, J. Molina-Perez²⁹, J. Monk⁷⁷, E. Monnier⁸³, S. Montesano^{89a,89b},
 F. Monticelli⁷⁰, S. Monzani^{19a,19b}, R.W. Moore², G.F. Moorhead⁸⁶, C. Mora Herrera⁴⁹, A. Moraes⁵³,
 N. Morange¹³⁶, J. Morel⁵⁴, G. Morello^{36a,36b}, D. Moreno⁸¹, M. Moreno Llácer¹⁶⁷, P. Morettini^{50a},
 M. Morgenstern⁴³, M. Morii⁵⁷, J. Morin⁷⁵, A.K. Morley²⁹, G. Mornacchi²⁹, J.D. Morris⁷⁵, L. Morvaj¹⁰¹,
 H.G. Moser⁹⁹, M. Mosidze^{51b}, J. Moss¹⁰⁹, R. Mount¹⁴³, E. Mountricha^{9,x}, S.V. Mouraviev⁹⁴,
 E.J.W. Moyses⁸⁴, F. Mueller^{58a}, J. Mueller¹²³, K. Mueller²⁰, T.A. Müller⁹⁸, T. Mueller⁸¹,
 D. Muenstermann²⁹, Y. Munwes¹⁵³, W.J. Murray¹²⁹, I. Mussche¹⁰⁵, E. Musto^{102a,102b}, A.G. Myagkov¹²⁸,
 M. Myska¹²⁵, J. Nadal¹¹, K. Nagai¹⁶⁰, K. Nagano⁶⁵, A. Nagarkar¹⁰⁹, Y. Nagasaka⁵⁹, M. Nagel⁹⁹,
 A.M. Nairz²⁹, Y. Nakahama²⁹, K. Nakamura¹⁵⁵, T. Nakamura¹⁵⁵, I. Nakano¹¹⁰, G. Nanava²⁰,
 A. Napier¹⁶¹, R. Narayan^{58b}, M. Nash^{77,c}, T. Nattermann²⁰, T. Naumann⁴¹, G. Navarro¹⁶², H.A. Neal⁸⁷,
 P.Yu. Nechaeva⁹⁴, T.J. Neep⁸², A. Negri^{119a,119b}, G. Negri²⁹, S. Nektarijevic⁴⁹, A. Nelson¹⁶³,
 T.K. Nelson¹⁴³, S. Nemecek¹²⁵, P. Nemethy¹⁰⁸, A.A. Nepomuceno^{23a}, M. Nessi^{29,y}, M.S. Neubauer¹⁶⁵,
 A. Neusiedl⁸¹, R.M. Neves¹⁰⁸, P. Nevski²⁴, P.R. Newman¹⁷, V. Nguyen Thi Hong¹³⁶, R.B. Nickerson¹¹⁸,
 R. Nicolaidou¹³⁶, B. Nicquevert²⁹, F. Niedercorn¹¹⁵, J. Nielsen¹³⁷, N. Nikiforou³⁴, A. Nikiforov¹⁵,
 V. Nikolaenko¹²⁸, I. Nikolic-Audit⁷⁸, K. Nikolics⁴⁹, K. Nikolopoulos²⁴, H. Nilsen⁴⁸, P. Nilsson⁷,
 Y. Ninomiya¹⁵⁵, A. Nisati^{132a}, T. Nishiyama⁶⁶, R. Nisius⁹⁹, L. Nodulman⁵, M. Nomachi¹¹⁶, I. Nomidis¹⁵⁴,
 M. Nordberg²⁹, P.R. Norton¹²⁹, J. Novakova¹²⁶, M. Nozaki⁶⁵, L. Nozka¹¹³, I.M. Nugent^{159a},
 A.-E. Nuncio-Quiroz²⁰, G. Nunes Hanninger⁸⁶, T. Nunnemann⁹⁸, E. Nurse⁷⁷, B.J. O'Brien⁴⁵,
 S.W. O'Neale^{17,*}, D.C. O'Neil¹⁴², V. O'Shea⁵³, L.B. Oakes⁹⁸, F.G. Oakham^{28,d}, H. Oberlack⁹⁹, J. Ocariz⁷⁸,
 A. Ochi⁶⁶, S. Oda⁶⁹, S. Odaka⁶⁵, J. Odier⁸³, H. Ogren⁶⁰, A. Oh⁸², S.H. Oh⁴⁴, C.C. Ohm^{146a,146b},
 T. Ohshima¹⁰¹, S. Okada⁶⁶, H. Okawa¹⁶³, Y. Okumura¹⁰¹, T. Okuyama¹⁵⁵, A. Olariu^{25a}, A.G. Olchevski⁶⁴,
 S.A. Olivares Pino^{31a}, M. Oliveira^{124a,h}, D. Oliveira Damazio²⁴, E. Oliver Garcia¹⁶⁷, D. Olivito¹²⁰,
 A. Olszewski³⁸, J. Olszowska³⁸, A. Onofre^{124a,z}, P.U.E. Onyisi³⁰, C.J. Oram^{159a}, M.J. Oreglia³⁰, Y. Oren¹⁵³,
 D. Orestano^{134a,134b}, N. Orlando^{72a,72b}, I. Orlov¹⁰⁷, C. Oropeza Barrera⁵³, R.S. Orr¹⁵⁸, B. Osculati^{50a,50b},

R. Ospanov¹²⁰, C. Osuna¹¹, G. Otero y Garzon²⁶, J.P. Ottersbach¹⁰⁵, M. Ouchrif^{135d}, E.A. Ouellette¹⁶⁹, F. Ould-Saada¹¹⁷, A. Ouraou¹³⁶, Q. Ouyang^{32a}, A. Ovcharova¹⁴, M. Owen⁸², S. Owen¹³⁹, V.E. Ozcan^{18a}, N. Ozturk⁷, A. Pacheco Pages¹¹, C. Padilla Aranda¹¹, S. Pagan Griso¹⁴, E. Paganis¹³⁹, F. Paige²⁴, P. Pais⁸⁴, K. Pajchel¹¹⁷, G. Palacino^{159b}, C.P. Paleari⁶, S. Palestini²⁹, D. Pallin³³, A. Palma^{124a}, J.D. Palmer¹⁷, Y.B. Pan¹⁷³, E. Panagiotopoulou⁹, P. Pani¹⁰⁵, N. Panikashvili⁸⁷, S. Panitkin²⁴, D. Pantea^{25a}, A. Papadelis^{146a}, Th.D. Papadopoulou⁹, A. Paramonov⁵, D. Paredes Hernandez³³, W. Park^{24,aa}, M.A. Parker²⁷, F. Parodi^{50a,50b}, J.A. Parsons³⁴, U. Parzefall⁴⁸, S. Pashapour⁵⁴, E. Pasqualucci^{132a}, S. Passaggio^{50a}, A. Passeri^{134a}, F. Pastore^{134a,134b}, Fr. Pastore⁷⁶, G. Pásztor^{49,ab}, S. Pataria¹⁷⁵, N. Patel¹⁵⁰, J.R. Pater⁸², S. Patricelli^{102a,102b}, T. Pauly²⁹, M. Pecsny^{144a}, M.I. Pedraza Morales¹⁷³, S.V. Peleganchuk¹⁰⁷, D. Pelikan¹⁶⁶, H. Peng^{32b}, B. Penning³⁰, A. Penson³⁴, J. Penwell⁶⁰, M. Perantoni^{23a}, K. Perez^{34,ac}, T. Perez Cavalcanti⁴¹, E. Perez Codina^{159a}, M.T. Pérez García-Estañ¹⁶⁷, V. Perez Reale³⁴, L. Perini^{89a,89b}, H. Pernegger²⁹, R. Perrino^{72a}, P. Perrodo⁴, S. Persema^{3a}, V.D. Peshekhonov⁶⁴, K. Peters²⁹, B.A. Petersen²⁹, J. Petersen²⁹, T.C. Petersen³⁵, E. Petit⁴, A. Petridis¹⁵⁴, C. Petridou¹⁵⁴, E. Petrolo^{132a}, F. Petrucci^{134a,134b}, D. Petschull⁴¹, M. Petteni¹⁴², R. Pezoa^{31b}, A. Phan⁸⁶, P.W. Phillips¹²⁹, G. Piacquadio²⁹, A. Picazio⁴⁹, E. Piccaro⁷⁵, M. Piccinini^{19a,19b}, S.M. Piec⁴¹, R. Piegai²⁶, D.T. Pignotti¹⁰⁹, J.E. Pilcher³⁰, A.D. Pilkington⁸², J. Pina^{124a,b}, M. Pinamonti^{164a,164c}, A. Pinder¹¹⁸, J.L. Pinfold², B. Pinto^{124a}, C. Pizio^{89a,89b}, M. Plamondon¹⁶⁹, M.-A. Pleier²⁴, E. Plotnikova⁶⁴, A. Poblaguev²⁴, S. Poddar^{58a}, F. Podlyski³³, L. Poggioli¹¹⁵, T. Poghosyan²⁰, M. Pohl⁴⁹, F. Polci⁵⁵, G. Polesello^{119a}, A. Policicchio^{36a,36b}, A. Polini^{19a}, J. Poll⁷⁵, V. Polychronakos²⁴, D.M. Pomarede¹³⁶, D. Pomeroy²², K. Pommès²⁹, L. Pontecorvo^{132a}, B.G. Pope⁸⁸, G.A. Popeneciu^{25a}, D.S. Popovic^{12a}, A. Poppleton²⁹, X. Portell Bueso²⁹, G.E. Pospelov⁹⁹, S. Pospisil¹²⁷, I.N. Potrap⁹⁹, C.J. Potter¹⁴⁹, C.T. Potter¹¹⁴, G. Poulard²⁹, J. Poveda¹⁷³, V. Pozdnyakov⁶⁴, R. Prabhu⁷⁷, P. Pralavorio⁸³, A. Pranko¹⁴, S. Prasad²⁹, R. Pravahan²⁴, S. Prell⁶³, K. Pretzl¹⁶, D. Price⁶⁰, J. Price⁷³, L.E. Price⁵, D. Prieur¹²³, M. Primavera^{72a}, K. Prokofiev¹⁰⁸, F. Prokoshin^{31b}, S. Protopopescu²⁴, J. Proudfoot⁵, X. Prudent⁴³, M. Przybycien³⁷, H. Przysiezniak⁴, S. Psoroulas²⁰, E. Ptacek¹¹⁴, E. Pueschel⁸⁴, J. Purdham⁸⁷, M. Purohit^{24,aa}, P. Puzo¹¹⁵, Y. Pylypchenko⁶², J. Qian⁸⁷, A. Quadt⁵⁴, D.R. Quarrie¹⁴, W.B. Quayle¹⁷³, F. Quinonez^{31a}, M. Raas¹⁰⁴, V. Radescu⁴¹, P. Radloff¹¹⁴, T. Rador^{18a}, F. Ragusa^{89a,89b}, G. Rahal¹⁷⁸, A.M. Rahimi¹⁰⁹, D. Rahm²⁴, S. Rajagopalan²⁴, M. Rammensee⁴⁸, M. Rammes¹⁴¹, A.S. Randle-Conde³⁹, K. Randrianarivony²⁸, F. Rauscher⁹⁸, T.C. Rave⁴⁸, M. Raymond²⁹, A.L. Read¹¹⁷, D.M. Rebuffi^{119a,119b}, A. Redelbach¹⁷⁴, G. Redlinger²⁴, R. Reece¹²⁰, K. Reeves⁴⁰, E. Reinherz-Aronis¹⁵³, A. Reinsch¹¹⁴, I. Reisinger⁴², C. Rembser²⁹, Z.L. Ren¹⁵¹, A. Renaud¹¹⁵, M. Rescigno^{132a}, S. Resconi^{89a}, B. Resende¹³⁶, P. Reznicek⁹⁸, R. Rezvani¹⁵⁸, R. Richter⁹⁹, E. Richter-Was^{4,ad}, M. Ridel⁷⁸, M. Rijpstra¹⁰⁵, M. Rijssenbeek¹⁴⁸, A. Rimoldi^{119a,119b}, L. Rinaldi^{19a}, R.R. Rios³⁹, I. Riu¹¹, G. Rivoltella^{89a,89b}, F. Rizatdinova¹¹², E. Rizvi⁷⁵, S.H. Robertson^{85,j}, A. Robichaud-Veronneau¹¹⁸, D. Robinson²⁷, J.E.M. Robinson⁷⁷, A. Robson⁵³, J.G. Rocha de Lima¹⁰⁶, C. Roda^{122a,122b}, D. Roda Dos Santos²⁹, D. Rodriguez¹⁶², A. Roe⁵⁴, S. Roe²⁹, O. Røhne¹¹⁷, S. Rolli¹⁶¹, A. Romaniouk⁹⁶, M. Romano^{19a,19b}, G. Romeo²⁶, E. Romero Adam¹⁶⁷, L. Roos⁷⁸, E. Ros¹⁶⁷, S. Rosati^{132a}, K. Rosbach⁴⁹, A. Rose¹⁴⁹, M. Rose⁷⁶, G.A. Rosenbaum¹⁵⁸, E.I. Rosenberg⁶³, P.L. Rosendahl¹³, O. Rosenthal¹⁴¹, L. Rossette⁴⁹, V. Rossetti¹¹, E. Rossi^{132a,132b}, L.P. Rossi^{50a}, M. Rotaru^{25a}, I. Roth¹⁷², J. Rothberg¹³⁸, D. Rousseau¹¹⁵, C.R. Royon¹³⁶, A. Rozanov⁸³, Y. Rozen¹⁵², X. Ruan^{32a,ae}, F. Rubbo¹¹, I. Rubinskiy⁴¹, B. Ruckert⁹⁸, N. Ruckstuhl¹⁰⁵, V.I. Rud⁹⁷, C. Rudolph⁴³, G. Rudolph⁶¹, F. Rühr⁶, F. Ruggieri^{134a,134b}, A. Ruiz-Martinez⁶³, L. Rummyantsev⁶⁴, K. Runge⁴⁸, Z. Rurikova⁴⁸, N.A. Rusakovich⁶⁴, J.P. Rutherford⁶, C. Ruwiedel¹⁴, P. Ruzicka¹²⁵, Y.F. Ryabov¹²¹, P. Ryan⁸⁸, M. Rybar¹²⁶, G. Rybkin¹¹⁵, N.C. Ryder¹¹⁸, A.F. Saavedra¹⁵⁰, I. Sadeh¹⁵³, H.F.-W. Sadrozinski¹³⁷, R. Sadykov⁶⁴, F. Safai Tehrani^{132a}, H. Sakamoto¹⁵⁵, G. Salamanna⁷⁵, A. Salamon^{133a}, M. Saleem¹¹¹, D. Salek²⁹, D. Salihagic⁹⁹, A. Salnikov¹⁴³, J. Salt¹⁶⁷, B.M. Salvachua Ferrando⁵, D. Salvatore^{36a,36b}, F. Salvatore¹⁴⁹, A. Salvucci¹⁰⁴, A. Salzburger²⁹, D. Sampsonidis¹⁵⁴, B.H. Samset¹¹⁷, A. Sanchez^{102a,102b}, V. Sanchez Martinez¹⁶⁷, H. Sandaker¹³, H.G. Sander⁸¹, M.P. Sanders⁹⁸, M. Sandhoff¹⁷⁵, T. Sandoval²⁷, C. Sandoval¹⁶², R. Sandstroem⁹⁹, D.P.C. Sankey¹²⁹, A. Sansoni⁴⁷, C. Santamarina Rios⁸⁵, C. Santoni³³, R. Santonico^{133a,133b}, H. Santos^{124a}, J.G. Saraiva^{124a}, T. Sarangi¹⁷³, E. Sarkisyan-Grinbaum⁷, F. Sarri^{122a,122b}, G. Sartisohn¹⁷⁵, O. Sasaki⁶⁵, N. Sasao⁶⁷, I. Satsounkevitch⁹⁰, G. Sauvage⁴, E. Sauvan⁴, J.B. Sauvan¹¹⁵, P. Savard^{158,d}, V. Savinov¹²³, D.O. Savu²⁹, L. Sawyer^{24,i}, D.H. Saxon⁵³, J. Saxon¹²⁰, C. Sbarra^{19a}, A. Sbrizzi^{19a,19b}, O. Scallion⁹³, D.A. Scannicchio¹⁶³,

M. Scarcella¹⁵⁰, J. Schaarschmidt¹¹⁵, P. Schacht⁹⁹, D. Schaefer¹²⁰, U. Schäfer⁸¹, S. Schaepe²⁰,
 S. Schaetzel^{58b}, A.C. Schaffer¹¹⁵, D. Schaile⁹⁸, R.D. Schamberger¹⁴⁸, A.G. Schamov¹⁰⁷, V. Scharf^{58a},
 V.A. Schegelsky¹²¹, D. Scheirich⁸⁷, M. Schernau¹⁶³, M.I. Scherzer³⁴, C. Schiavi^{50a,50b}, J. Schieck⁹⁸,
 M. Schioppa^{36a,36b}, S. Schlenker²⁹, E. Schmidt⁴⁸, K. Schmieden²⁰, C. Schmitt⁸¹, S. Schmitt^{58b},
 M. Schmitz²⁰, B. Schneider¹⁶, U. Schnoor⁴³, A. Schöning^{58b}, M. Schott²⁹, D. Schouten^{159a},
 J. Schovancova¹²⁵, M. Schram⁸⁵, C. Schroeder⁸¹, N. Schroer^{58c}, M.J. Schultens²⁰, J. Schultes¹⁷⁵,
 H.-C. Schultz-Coulon^{58a}, H. Schulz¹⁵, J.W. Schumacher²⁰, M. Schumacher⁴⁸, B.A. Schumm¹³⁷,
 Ph. Schune¹³⁶, C. Schwanenberger⁸², A. Schwartzman¹⁴³, Ph. Schwemling⁷⁸, R. Schwienhorst⁸⁸,
 R. Schwierz⁴³, J. Schwindling¹³⁶, T. Schwindt²⁰, M. Schwoerer⁴, G. Sciolla²², W.G. Scott¹²⁹, J. Searcy¹¹⁴,
 G. Sedov⁴¹, E. Sedykh¹²¹, S.C. Seidel¹⁰³, A. Seiden¹³⁷, F. Seifert⁴³, J.M. Seixas^{23a}, G. Sekhniaidze^{102a},
 S.J. Sekula³⁹, K.E. Selbach⁴⁵, D.M. Seliverstov¹²¹, B. Sellden^{146a}, G. Sellers⁷³, M. Seman^{144b},
 N. Semprini-Cesari^{19a,19b}, C. Serfon⁹⁸, L. Serin¹¹⁵, L. Serkin⁵⁴, R. Seuster⁹⁹, H. Severini¹¹¹, A. Sfyrla²⁹,
 E. Shabalina⁵⁴, M. Shamim¹¹⁴, L.Y. Shan^{32a}, J.T. Shank²¹, Q.T. Shao⁸⁶, M. Shapiro¹⁴, P.B. Shatalov⁹⁵,
 K. Shaw^{164a,164c}, D. Sherman¹⁷⁶, P. Sherwood⁷⁷, A. Shibata¹⁰⁸, H. Shichi¹⁰¹, S. Shimizu²⁹,
 M. Shimojima¹⁰⁰, T. Shin⁵⁶, M. Shiyakova⁶⁴, A. Shmeleva⁹⁴, M.J. Shochet³⁰, D. Short¹¹⁸, S. Shrestha⁶³,
 E. Shulga⁹⁶, M.A. Shupe⁶, P. Sicho¹²⁵, A. Sidoti^{132a}, F. Siegert⁴⁸, Dj. Sijacki^{12a}, O. Silbert¹⁷², J. Silva^{124a},
 Y. Silver¹⁵³, D. Silverstein¹⁴³, S.B. Silverstein^{146a}, V. Simak¹²⁷, O. Simard¹³⁶, Lj. Simic^{12a}, S. Simion¹¹⁵,
 B. Simmons⁷⁷, R. Simoniello^{89a,89b}, M. Simonyan³⁵, P. Sinervo¹⁵⁸, N.B. Sinev¹¹⁴, V. Sipica¹⁴¹,
 G. Siragusa¹⁷⁴, A. Sircar²⁴, A.N. Sisakyan⁶⁴, S.Yu. Sivoklov⁹⁷, J. Sjölin^{146a,146b}, T.B. Sjusen¹³,
 L.A. Skinnari¹⁴, H.P. Skottowe⁵⁷, K. Skovpen¹⁰⁷, P. Skubic¹¹¹, M. Slater¹⁷, T. Slavicek¹²⁷, K. Sliwa¹⁶¹,
 V. Smakhtin¹⁷², B.H. Smart⁴⁵, S.Yu. Smirnov⁹⁶, Y. Smirnov⁹⁶, L.N. Smirnova⁹⁷, O. Smirnova⁷⁹,
 B.C. Smith⁵⁷, D. Smith¹⁴³, K.M. Smith⁵³, M. Smizanska⁷¹, K. Smolek¹²⁷, A.A. Snesev⁹⁴, S.W. Snow⁸²,
 J. Snow¹¹¹, S. Snyder²⁴, R. Sobie^{169j}, J. Sodomka¹²⁷, A. Soffer¹⁵³, C.A. Solans¹⁶⁷, M. Solar¹²⁷, J. Solc¹²⁷,
 E. Soldatov⁹⁶, U. Soldevila¹⁶⁷, E. Solfaroli Camillocci^{132a,132b}, A.A. Solodkov¹²⁸, O.V. Solovyanov¹²⁸,
 N. Soni², V. Sopko¹²⁷, B. Sopko¹²⁷, M. Sosebee⁷, R. Soualah^{164a,164c}, A. Soukharev¹⁰⁷,
 S. Spagnolo^{72a,72b}, F. Spanò⁷⁶, R. Spighi^{19a}, G. Spigo²⁹, F. Spila^{132a,132b}, R. Spiwoks²⁹, M. Spousta¹²⁶,
 T. Spreitzer¹⁵⁸, B. Spurlock⁷, R.D. St. Denis⁵³, J. Stahlman¹²⁰, R. Stamen^{58a}, E. Stanecka³⁸, R.W. Stanek⁵,
 C. Stanescu^{134a}, M. Stanescu-Bellu⁴¹, S. Stapnes¹¹⁷, E.A. Starchenko¹²⁸, J. Stark⁵⁵, P. Staroba¹²⁵,
 P. Starovoitov⁴¹, A. Staude⁹⁸, P. Stavina^{144a}, G. Steele⁵³, P. Steinbach⁴³, P. Steinberg²⁴, I. Stekl¹²⁷,
 B. Stelzer¹⁴², H.J. Stelzer⁸⁸, O. Stelzer-Chilton^{159a}, H. Stenzel⁵², S. Stern⁹⁹, G.A. Stewart²⁹,
 J.A. Stillings²⁰, M.C. Stockton⁸⁵, K. Stoerig⁴⁸, G. Stoicea^{25a}, S. Stonjek⁹⁹, P. Strachota¹²⁶, A.R. Stradling⁷,
 A. Straessner⁴³, J. Strandberg¹⁴⁷, S. Strandberg^{146a,146b}, A. Strandlie¹¹⁷, M. Strang¹⁰⁹, E. Strauss¹⁴³,
 M. Strauss¹¹¹, P. Strizenec^{144b}, R. Ströhmer¹⁷⁴, D.M. Strom¹¹⁴, J.A. Strong^{76,*}, R. Stroynowski³⁹,
 J. Strube¹²⁹, B. Stugu¹³, I. Stumer^{24,*}, J. Stupak¹⁴⁸, P. Sturm¹⁷⁵, N.A. Styles⁴¹, D.A. Soh^{151,u}, D. Su¹⁴³,
 HS. Subramania², A. Succurro¹¹, Y. Sugaya¹¹⁶, C. Suhr¹⁰⁶, K. Suita⁶⁶, M. Suk¹²⁶, V.V. Sulin⁹⁴,
 S. Sultansoy^{3d}, T. Sumida⁶⁷, X. Sun⁵⁵, J.E. Sundermann⁴⁸, K. Suruliz¹³⁹, G. Susinno^{36a,36b},
 M.R. Sutton¹⁴⁹, Y. Suzuki⁶⁵, Y. Suzuki⁶⁶, M. Svatos¹²⁵, S. Swedish¹⁶⁸, I. Sykora^{144a}, T. Sykora¹²⁶,
 J. Sánchez¹⁶⁷, D. Ta¹⁰⁵, K. Tackmann⁴¹, A. Taffard¹⁶³, R. Tafirot^{159a}, N. Taiblum¹⁵³, Y. Takahashi¹⁰¹,
 H. Takai²⁴, R. Takashima⁶⁸, H. Takeda⁶⁶, T. Takeshita¹⁴⁰, Y. Takubo⁶⁵, M. Talby⁸³, A. Talyshev^{107,f},
 M.C. Tamsett²⁴, J. Tanaka¹⁵⁵, R. Tanaka¹¹⁵, S. Tanaka¹³¹, S. Tanaka⁶⁵, A.J. Tanasijczuk¹⁴², K. Tani⁶⁶,
 N. Tannoury⁸³, S. Tapprogge⁸¹, D. Tardif¹⁵⁸, S. Tarem¹⁵², F. Tarrade²⁸, G.F. Tartarelli^{89a}, P. Tas¹²⁶,
 M. Tasevsky¹²⁵, E. Tassi^{36a,36b}, M. Tatarkhanov¹⁴, Y. Tayalati^{135d}, C. Taylor⁷⁷, F.E. Taylor⁹²,
 G.N. Taylor⁸⁶, W. Taylor^{159b}, M. Teinturier¹¹⁵, M. Teixeira Dias Castanheira⁷⁵, P. Teixeira-Dias⁷⁶,
 K.K. Temming⁴⁸, H. Ten Kate²⁹, P.K. Teng¹⁵¹, S. Terada⁶⁵, K. Terashi¹⁵⁵, J. Terron⁸⁰, M. Testa⁴⁷,
 R.J. Teuscher^{158,j}, J. Therhaag²⁰, T. Theveneaux-Pelzer⁷⁸, M. Thioye¹⁷⁶, S. Thoma⁴⁸, J.P. Thomas¹⁷,
 E.N. Thompson³⁴, P.D. Thompson¹⁷, P.D. Thompson¹⁵⁸, A.S. Thompson⁵³, L.A. Thomsen³⁵,
 E. Thomson¹²⁰, M. Thomson²⁷, R.P. Thun⁸⁷, F. Tian³⁴, M.J. Tibbetts¹⁴, T. Tic¹²⁵, V.O. Tikhomirov⁹⁴,
 Y.A. Tikhonov^{107,f}, S. Timoshenko⁹⁶, P. Tipton¹⁷⁶, F.J. Tique Aires Viegas²⁹, S. Tisserant⁸³, T. Todorov⁴,
 S. Todorova-Nova¹⁶¹, B. Toggerson¹⁶³, J. Tojo⁶⁹, S. Tokár^{144a}, K. Tokunaga⁶⁶, K. Tokushuku⁶⁵,
 K. Tollefson⁸⁸, M. Tomoto¹⁰¹, L. Tompkins³⁰, K. Toms¹⁰³, A. Tonoyan¹³, C. Topfel¹⁶, N.D. Topilin⁶⁴,
 I. Torchiani²⁹, E. Torrence¹¹⁴, H. Torres⁷⁸, E. Torró Pastor¹⁶⁷, J. Toth^{83,ab}, F. Touchard⁸³, D.R. Tovey¹³⁹,
 T. Trefzger¹⁷⁴, L. Tremblet²⁹, A. Tricoli²⁹, I.M. Trigger^{159a}, S. Trincaz-Duvold⁷⁸, M.F. Tripiana⁷⁰,

W. Trischuk¹⁵⁸, B. Trocmé⁵⁵, C. Troncon^{89a}, M. Trottier-McDonald¹⁴², M. Trzebinski³⁸, A. Trzupek³⁸, C. Tsarouchas²⁹, J.C.-L. Tseng¹¹⁸, M. Tsiakiris¹⁰⁵, P.V. Tsiarehsha⁹⁰, D. Tsiou^{4,af}, G. Tsipolitis⁹, V. Tsiskaridze⁴⁸, E.G. Tskhadadze^{51a}, I.I. Tsukerman⁹⁵, V. Tsulaia¹⁴, J.-W. Tsung²⁰, S. Tsuno⁶⁵, D. Tsybychev¹⁴⁸, A. Tua¹³⁹, A. Tudorache^{25a}, V. Tudorache^{25a}, J.M. Tuggle³⁰, M. Turala³⁸, D. Turecek¹²⁷, I. Turk Cakir^{3e}, E. Turlay¹⁰⁵, R. Turra^{89a,89b}, P.M. Tuts³⁴, A. Tykhonov⁷⁴, M. Tylmad^{146a,146b}, M. Tyndel¹²⁹, G. Tzanakos⁸, K. Uchida²⁰, I. Ueda¹⁵⁵, R. Ueno²⁸, M. Ugland¹³, M. Uhlenbrock²⁰, M. Uhrmacher⁵⁴, F. Ukegawa¹⁶⁰, G. Unal²⁹, A. Undrus²⁴, G. Unel¹⁶³, Y. Unno⁶⁵, D. Urbaniec³⁴, G. Usai⁷, M. Uslenghi^{119a,119b}, L. Vacavant⁸³, V. Vacek¹²⁷, B. Vachon⁸⁵, S. Vahsen¹⁴, J. Valenta¹²⁵, P. Valente^{132a}, S. Valentinetti^{19a,19b}, S. Valkar¹²⁶, E. Valladolid Gallego¹⁶⁷, S. Vallecorsa¹⁵², J.A. Valls Ferrer¹⁶⁷, H. van der Graaf¹⁰⁵, E. van der Kraaij¹⁰⁵, R. Van Der Leeuw¹⁰⁵, E. van der Poel¹⁰⁵, D. van der Ster²⁹, N. van Eldik⁸⁴, P. van Gemmeren⁵, I. van Vulpen¹⁰⁵, M. Vanadia⁹⁹, W. Vandelli²⁹, A. Vaniachine⁵, P. Vankov⁴¹, F. Vannucci⁷⁸, R. Vari^{132a}, T. Varol⁸⁴, D. Varouchas¹⁴, A. Vartapetian⁷, K.E. Varvell¹⁵⁰, V.I. Vassilakopoulos⁵⁶, F. Vazeille³³, T. Vazquez Schroeder⁵⁴, G. Vegni^{89a,89b}, J.J. Veillet¹¹⁵, F. Veloso^{124a}, R. Veness²⁹, S. Veneziano^{132a}, A. Ventura^{72a,72b}, D. Ventura⁸⁴, M. Venturi⁴⁸, N. Venturi¹⁵⁸, V. Vercesi^{119a}, M. Verducci¹³⁸, W. Verkerke¹⁰⁵, J.C. Vermeulen¹⁰⁵, A. Vest⁴³, M.C. Vetterli^{142,d}, I. Vichou¹⁶⁵, T. Vickey^{145b,ag}, O.E. Vickey Boeriu^{145b}, G.H.A. Viehhauser¹¹⁸, S. Viel¹⁶⁸, M. Villa^{19a,19b}, M. Villaplana Perez¹⁶⁷, E. Vilucchi⁴⁷, M.G. Vincker²⁸, E. Vinek²⁹, V.B. Vinogradov⁶⁴, M. Virchaux^{136,*}, J. Virzi¹⁴, O. Vitells¹⁷², M. Viti⁴¹, I. Vivarelli⁴⁸, F. Vives Vaque², S. Vlachos⁹, D. Vladoiu⁹⁸, M. Vlasak¹²⁷, A. Vogel²⁰, P. Vokac¹²⁷, G. Volpi⁴⁷, M. Volpi⁸⁶, G. Volpini^{89a}, H. von der Schmitt⁹⁹, J. von Loeben⁹⁹, H. von Radziewski⁴⁸, E. von Toerne²⁰, V. Vorobel¹²⁶, V. Vorwerk¹¹, M. Vos¹⁶⁷, R. Voss²⁹, T.T. Voss¹⁷⁵, J.H. Vosseveld⁷³, N. Vranjes¹³⁶, M. Vranjes Milosavljevic¹⁰⁵, V. Vrba¹²⁵, M. Vreeswijk¹⁰⁵, T. Vu Anh⁴⁸, R. Vuillermet²⁹, I. Vukotic¹¹⁵, W. Wagner¹⁷⁵, P. Wagner¹²⁰, H. Wahlen¹⁷⁵, S. Wahrmund⁴³, J. Wakabayashi¹⁰¹, S. Walch⁸⁷, J. Walder⁷¹, R. Walker⁹⁸, W. Walkowiak¹⁴¹, R. Wall¹⁷⁶, P. Waller⁷³, C. Wang⁴⁴, H. Wang¹⁷³, H. Wang^{32b,ah}, J. Wang¹⁵¹, J. Wang⁵⁵, J.C. Wang¹³⁸, R. Wang¹⁰³, S.M. Wang¹⁵¹, T. Wang²⁰, A. Warburton⁸⁵, C.P. Ward²⁷, M. Warsinsky⁴⁸, A. Washbrook⁴⁵, C. Wasicki⁴¹, P.M. Watkins¹⁷, A.T. Watson¹⁷, I.J. Watson¹⁵⁰, M.F. Watson¹⁷, G. Watts¹³⁸, S. Watts⁸², A.T. Waugh¹⁵⁰, B.M. Waugh⁷⁷, M. Weber¹²⁹, M.S. Weber¹⁶, P. Weber⁵⁴, A.R. Weidberg¹¹⁸, P. Weigell⁹⁹, J. Weingarten⁵⁴, C. Weiser⁴⁸, H. Wellenstein²², P.S. Wells²⁹, T. Wenaus²⁴, D. Wendland¹⁵, Z. Weng^{151,u}, T. Wengler²⁹, S. Wenig²⁹, N. Wermes²⁰, M. Werner⁴⁸, P. Werner²⁹, M. Werth¹⁶³, M. Wessels^{58a}, J. Wetter¹⁶¹, C. Weydert⁵⁵, K. Whalen²⁸, S.J. Wheeler-Ellis¹⁶³, A. White⁷, M.J. White⁸⁶, S. White^{122a,122b}, S.R. Whitehead¹¹⁸, D. Whiteson¹⁶³, D. Whittington⁶⁰, F. Wicek¹¹⁵, D. Wicke¹⁷⁵, F.J. Wickens¹²⁹, W. Wiedenmann¹⁷³, M. Wielers¹²⁹, P. Wienemann²⁰, C. Wiglesworth⁷⁵, L.A.M. Wiik-Fuchs⁴⁸, P.A. Wijeratne⁷⁷, A. Wildauer¹⁶⁷, M.A. Wildt^{41,q}, I. Wilhelm¹²⁶, H.G. Wilkens²⁹, J.Z. Will⁹⁸, E. Williams³⁴, H.H. Williams¹²⁰, W. Willis³⁴, S. Willocq⁸⁴, J.A. Wilson¹⁷, M.G. Wilson¹⁴³, A. Wilson⁸⁷, I. Wingerter-Seez⁴, S. Winkelmann⁴⁸, F. Winklmeier²⁹, M. Wittgen¹⁴³, M.W. Wolter³⁸, H. Wolters^{124a,h}, W.C. Wong⁴⁰, G. Wooden⁸⁷, B.K. Wosiek³⁸, J. Wotschack²⁹, M.J. Woudstra⁸⁴, K.W. Wozniak³⁸, K. Wraight⁵³, C. Wright⁵³, M. Wright⁵³, B. Wrona⁷³, S.L. Wu¹⁷³, X. Wu⁴⁹, Y. Wu^{32b,ai}, E. Wulf³⁴, B.M. Wynne⁴⁵, S. Xella³⁵, M. Xiao¹³⁶, S. Xie⁴⁸, C. Xu^{32b,x}, D. Xu¹³⁹, B. Yabsley¹⁵⁰, S. Yacoob^{145b}, M. Yamada⁶⁵, H. Yamaguchi¹⁵⁵, A. Yamamoto⁶⁵, K. Yamamoto⁶³, S. Yamamoto¹⁵⁵, T. Yamamura¹⁵⁵, T. Yamanaka¹⁵⁵, J. Yamaoka⁴⁴, T. Yamazaki¹⁵⁵, Y. Yamazaki⁶⁶, Z. Yan²¹, H. Yang⁸⁷, U.K. Yang⁸², Y. Yang⁶⁰, Z. Yang^{146a,146b}, S. Yanush⁹¹, L. Yao^{32a}, Y. Yao¹⁴, Y. Yasu⁶⁵, G.V. Ybeles Smit¹³⁰, J. Ye³⁹, S. Ye²⁴, M. Yilmaz^{3c}, R. Yoosoofmiya¹²³, K. Yorita¹⁷¹, R. Yoshida⁵, C. Young¹⁴³, C.J. Young¹¹⁸, S. Youssef²¹, D. Yu²⁴, J. Yu⁷, J. Yu¹¹², L. Yuan⁶⁶, A. Yurkewicz¹⁰⁶, B. Zabinski³⁸, R. Zaidan⁶², A.M. Zaitsev¹²⁸, Z. Zajacova²⁹, L. Zanello^{132a,132b}, A. Zaytsev¹⁰⁷, C. Zeitnitz¹⁷⁵, M. Zeller¹⁷⁶, M. Zeman¹²⁵, A. Zemla³⁸, C. Zender²⁰, O. Zenin¹²⁸, T. Ženiš^{144a}, Z. Zinonos^{122a,122b}, S. Zenz¹⁴, D. Zerwas¹¹⁵, G. Zevi della Porta⁵⁷, Z. Zhan^{32d}, D. Zhang^{32b,ah}, H. Zhang⁸⁸, J. Zhang⁵, X. Zhang^{32d}, Z. Zhang¹¹⁵, L. Zhao¹⁰⁸, T. Zhao¹³⁸, Z. Zhao^{32b}, A. Zhemchugov⁶⁴, J. Zhong¹¹⁸, B. Zhou⁸⁷, N. Zhou¹⁶³, Y. Zhou¹⁵¹, C.G. Zhu^{32d}, H. Zhu⁴¹, J. Zhu⁸⁷, Y. Zhu^{32b}, X. Zhuang⁹⁸, V. Zhuravlov⁹⁹, D. Zieminska⁶⁰, R. Zimmermann²⁰, S. Zimmermann²⁰, S. Zimmermann⁴⁸, M. Ziolkowski¹⁴¹, R. Zitoun⁴, L. Živković³⁴, V.V. Zmouchko^{128,*}, G. Zobernig¹⁷³, A. Zoccoli^{19a,19b}, M. zur Nedden¹⁵, V. Zutshi¹⁰⁶, L. Zwalinski²⁹

¹ University at Albany, Albany, NY, United States

- ² Department of Physics, University of Alberta, Edmonton AB, Canada
- ³ ^(a) Department of Physics, Ankara University, Ankara; ^(b) Department of Physics, Dumlupinar University, Kutahya; ^(c) Department of Physics, Gazi University, Ankara; ^(d) Division of Physics, TOBB University of Economics and Technology, Ankara; ^(e) Turkish Atomic Energy Authority, Ankara, Turkey
- ⁴ LAPP, CNRS/IN2P3 and Université de Savoie, Annecy-le-Vieux, France
- ⁵ High Energy Physics Division, Argonne National Laboratory, Argonne, IL, United States
- ⁶ Department of Physics, University of Arizona, Tucson, AZ, United States
- ⁷ Department of Physics, The University of Texas at Arlington, Arlington, TX, United States
- ⁸ Physics Department, University of Athens, Athens, Greece
- ⁹ Physics Department, National Technical University of Athens, Zografou, Greece
- ¹⁰ Institute of Physics, Azerbaijan Academy of Sciences, Baku, Azerbaijan
- ¹¹ Institut de Física d'Altes Energies and Departament de Física de la Universitat Autònoma de Barcelona and ICREA, Barcelona, Spain
- ¹² ^(a) Institute of Physics, University of Belgrade, Belgrade; ^(b) Vinca Institute of Nuclear Sciences, University of Belgrade, Belgrade, Serbia
- ¹³ Department for Physics and Technology, University of Bergen, Bergen, Norway
- ¹⁴ Physics Division, Lawrence Berkeley National Laboratory and University of California, Berkeley, CA, United States
- ¹⁵ Department of Physics, Humboldt University, Berlin, Germany
- ¹⁶ Albert Einstein Center for Fundamental Physics and Laboratory for High Energy Physics, University of Bern, Bern, Switzerland
- ¹⁷ School of Physics and Astronomy, University of Birmingham, Birmingham, United Kingdom
- ¹⁸ ^(a) Department of Physics, Bogazici University, Istanbul; ^(b) Division of Physics, Dogus University, Istanbul; ^(c) Department of Physics Engineering, Gaziantep University, Gaziantep;
- ^(d) Department of Physics, Istanbul Technical University, Istanbul, Turkey
- ¹⁹ ^(a) INFN Sezione di Bologna; ^(b) Dipartimento di Fisica, Università di Bologna, Bologna, Italy
- ²⁰ Physikalisches Institut, University of Bonn, Bonn, Germany
- ²¹ Department of Physics, Boston University, Boston, MA, United States
- ²² Department of Physics, Brandeis University, Waltham, MA, United States
- ²³ ^(a) Universidade Federal do Rio De Janeiro COPPE/EE/IF, Rio de Janeiro; ^(b) Federal University of Juiz de Fora (UFJF), Juiz de Fora; ^(c) Federal University of Sao Joao del Rei (UFSJ), Sao Joao del Rei; ^(d) Instituto de Física, Universidade de Sao Paulo, Sao Paulo, Brazil
- ²⁴ Physics Department, Brookhaven National Laboratory, Upton, NY, United States
- ²⁵ ^(a) National Institute of Physics and Nuclear Engineering, Bucharest; ^(b) University Politehnica Bucharest, Bucharest; ^(c) West University in Timisoara, Timisoara, Romania
- ²⁶ Departamento de Física, Universidad de Buenos Aires, Buenos Aires, Argentina
- ²⁷ Cavendish Laboratory, University of Cambridge, Cambridge, United Kingdom
- ²⁸ Department of Physics, Carleton University, Ottawa, ON, Canada
- ²⁹ CERN, Geneva, Switzerland
- ³⁰ Enrico Fermi Institute, University of Chicago, Chicago, IL, United States
- ³¹ ^(a) Departamento de Física, Pontificia Universidad Católica de Chile, Santiago; ^(b) Departamento de Física, Universidad Técnica Federico Santa María, Valparaíso, Chile
- ³² ^(a) Institute of High Energy Physics, Chinese Academy of Sciences, Beijing; ^(b) Department of Modern Physics, University of Science and Technology of China, Anhui; ^(c) Department of Physics, Nanjing University, Jiangsu; ^(d) School of Physics, Shandong University, Shandong, China
- ³³ Laboratoire de Physique Corpusculaire, Clermont Université and Université Blaise Pascal and CNRS/IN2P3, Aubiere Cedex, France
- ³⁴ Nevis Laboratory, Columbia University, Irvington, NY, United States
- ³⁵ Niels Bohr Institute, University of Copenhagen, Copenhagen, Denmark
- ³⁶ ^(a) INFN Gruppo Collegato di Cosenza; ^(b) Dipartimento di Fisica, Università della Calabria, Arcavata di Rende, Italy
- ³⁷ AGH University of Science and Technology, Faculty of Physics and Applied Computer Science, Krakow, Poland
- ³⁸ The Henryk Niewodniczanski Institute of Nuclear Physics, Polish Academy of Sciences, Krakow, Poland
- ³⁹ Physics Department, Southern Methodist University, Dallas, TX, United States
- ⁴⁰ Physics Department, University of Texas at Dallas, Richardson, TX, United States
- ⁴¹ DESY, Hamburg and Zeuthen, Germany
- ⁴² Institut für Experimentelle Physik IV, Technische Universität Dortmund, Dortmund, Germany
- ⁴³ Institut für Kern- und Teilchenphysik, Technical University Dresden, Dresden, Germany
- ⁴⁴ Department of Physics, Duke University, Durham, NC, United States
- ⁴⁵ SUPA - School of Physics and Astronomy, University of Edinburgh, Edinburgh, United Kingdom
- ⁴⁶ Fachhochschule Wiener Neustadt, Johannes Gutenbergstrasse 3 2700 Wiener Neustadt, Austria
- ⁴⁷ INFN Laboratori Nazionali di Frascati, Frascati, Italy
- ⁴⁸ Fakultät für Mathematik und Physik, Albert-Ludwigs-Universität, Freiburg i.Br., Germany
- ⁴⁹ Section de Physique, Université de Genève, Geneva, Switzerland
- ⁵⁰ ^(a) INFN Sezione di Genova; ^(b) Dipartimento di Fisica, Università di Genova, Genova, Italy
- ⁵¹ ^(a) E. Andronikashvili Institute of Physics, Tbilisi State University, Tbilisi; ^(b) High Energy Physics Institute, Tbilisi State University, Tbilisi, Georgia
- ⁵² II Physikalisches Institut, Justus-Liebig-Universität Giessen, Giessen, Germany
- ⁵³ SUPA - School of Physics and Astronomy, University of Glasgow, Glasgow, United Kingdom
- ⁵⁴ II Physikalisches Institut, Georg-August-Universität, Göttingen, Germany
- ⁵⁵ Laboratoire de Physique Subatomique et de Cosmologie, Université Joseph Fourier and CNRS/IN2P3 and Institut National Polytechnique de Grenoble, Grenoble, France
- ⁵⁶ Department of Physics, Hampton University, Hampton, VA, United States
- ⁵⁷ Laboratory for Particle Physics and Cosmology, Harvard University, Cambridge, MA, United States
- ⁵⁸ ^(a) Kirchhoff-Institut für Physik, Ruprecht-Karls-Universität Heidelberg, Heidelberg; ^(b) Physikalisches Institut, Ruprecht-Karls-Universität Heidelberg, Heidelberg; ^(c) ZITI Institut für technische Informatik, Ruprecht-Karls-Universität Heidelberg, Mannheim, Germany
- ⁵⁹ Faculty of Applied Information Science, Hiroshima Institute of Technology, Hiroshima, Japan
- ⁶⁰ Department of Physics, Indiana University, Bloomington, IN, United States
- ⁶¹ Institut für Astro- und Teilchenphysik, Leopold-Franzens-Universität, Innsbruck, Austria
- ⁶² University of Iowa, Iowa City, IA, United States
- ⁶³ Department of Physics and Astronomy, Iowa State University, Ames, IA, United States
- ⁶⁴ Joint Institute for Nuclear Research, JINR Dubna, Dubna, Russia
- ⁶⁵ KEK, High Energy Accelerator Research Organization, Tsukuba, Japan
- ⁶⁶ Graduate School of Science, Kobe University, Kobe, Japan
- ⁶⁷ Faculty of Science, Kyoto University, Kyoto, Japan
- ⁶⁸ Kyoto University of Education, Kyoto, Japan
- ⁶⁹ Department of Physics, Kyushu University, Fukuoka, Japan
- ⁷⁰ Instituto de Física La Plata, Universidad Nacional de La Plata and CONICET, La Plata, Argentina
- ⁷¹ Physics Department, Lancaster University, Lancaster, United Kingdom
- ⁷² ^(a) INFN Sezione di Lecce; ^(b) Dipartimento di Matematica e Fisica, Università del Salento, Lecce, Italy
- ⁷³ Oliver Lodge Laboratory, University of Liverpool, Liverpool, United Kingdom
- ⁷⁴ Department of Physics, Jožef Stefan Institute and University of Ljubljana, Ljubljana, Slovenia
- ⁷⁵ School of Physics and Astronomy, Queen Mary University of London, London, United Kingdom

- 76 Department of Physics, Royal Holloway University of London, Surrey, United Kingdom
- 77 Department of Physics and Astronomy, University College London, London, United Kingdom
- 78 Laboratoire de Physique Nucléaire et de Hautes Energies, UPMC and Université Paris-Diderot and CNRS/IN2P3, Paris, France
- 79 Fysiska institutionen, Lunds universitet, Lund, Sweden
- 80 Departamento de Física Teórica C-15, Universidad Autonoma de Madrid, Madrid, Spain
- 81 Institut für Physik, Universität Mainz, Mainz, Germany
- 82 School of Physics and Astronomy, University of Manchester, Manchester, United Kingdom
- 83 CPPM, Aix-Marseille Université and CNRS/IN2P3, Marseille, France
- 84 Department of Physics, University of Massachusetts, Amherst, MA, United States
- 85 Department of Physics, McGill University, Montreal, QC, Canada
- 86 School of Physics, University of Melbourne, Victoria, Australia
- 87 Department of Physics, The University of Michigan, Ann Arbor, MI, United States
- 88 Department of Physics and Astronomy, Michigan State University, East Lansing, MI, United States
- 89 ^(a) INFN Sezione di Milano; ^(b) Dipartimento di Fisica, Università di Milano, Milano, Italy
- 90 B.I. Stepanov Institute of Physics, National Academy of Sciences of Belarus, Minsk, Belarus
- 91 National Scientific and Educational Centre for Particle and High Energy Physics, Minsk, Belarus
- 92 Department of Physics, Massachusetts Institute of Technology, Cambridge, MA, United States
- 93 Group of Particle Physics, University of Montreal, Montreal, QC, Canada
- 94 P.N. Lebedev Institute of Physics, Academy of Sciences, Moscow, Russia
- 95 Institute for Theoretical and Experimental Physics (ITEP), Moscow, Russia
- 96 Moscow Engineering and Physics Institute (MEPhI), Moscow, Russia
- 97 Skobeltsyn Institute of Nuclear Physics, Lomonosov Moscow State University, Moscow, Russia
- 98 Fakultät für Physik, Ludwig-Maximilians-Universität München, München, Germany
- 99 Max-Planck-Institut für Physik (Werner-Heisenberg-Institut), München, Germany
- 100 Nagasaki Institute of Applied Science, Nagasaki, Japan
- 101 Graduate School of Science, Nagoya University, Nagoya, Japan
- 102 ^(a) INFN Sezione di Napoli; ^(b) Dipartimento di Scienze Fisiche, Università di Napoli, Napoli, Italy
- 103 Department of Physics and Astronomy, University of New Mexico, Albuquerque, NM, United States
- 104 Institute for Mathematics, Astrophysics and Particle Physics, Radboud University Nijmegen/Nikhef, Nijmegen, Netherlands
- 105 Nikhef National Institute for Subatomic Physics and University of Amsterdam, Amsterdam, Netherlands
- 106 Department of Physics, Northern Illinois University, DeKalb, IL, United States
- 107 Budker Institute of Nuclear Physics, SB RAS, Novosibirsk, Russia
- 108 Department of Physics, New York University, New York, NY, United States
- 109 Ohio State University, Columbus, OH, United States
- 110 Faculty of Science, Okayama University, Okayama, Japan
- 111 Homer L. Dodge Department of Physics and Astronomy, University of Oklahoma, Norman, OK, United States
- 112 Department of Physics, Oklahoma State University, Stillwater, OK, United States
- 113 Palacký University, RCPTM, Olomouc, Czech Republic
- 114 Center for High Energy Physics, University of Oregon, Eugene, OR, United States
- 115 LAL, Univ. Paris-Sud and CNRS/IN2P3, Orsay, France
- 116 Graduate School of Science, Osaka University, Osaka, Japan
- 117 Department of Physics, University of Oslo, Oslo, Norway
- 118 Department of Physics, Oxford University, Oxford, United Kingdom
- 119 ^(a) INFN Sezione di Pavia; ^(b) Dipartimento di Fisica, Università di Pavia, Pavia, Italy
- 120 Department of Physics, University of Pennsylvania, Philadelphia, PA, United States
- 121 Petersburg Nuclear Physics Institute, Gatchina, Russia
- 122 ^(a) INFN Sezione di Pisa; ^(b) Dipartimento di Fisica E. Fermi, Università di Pisa, Pisa, Italy
- 123 Department of Physics and Astronomy, University of Pittsburgh, Pittsburgh, PA, United States
- 124 ^(a) Laboratório de Instrumentação e Física Experimental de Partículas – LIP, Lisboa, Portugal; ^(b) Departamento de Física Teórica y del Cosmos and CAFPE, Universidad de Granada, Granada, Spain
- 125 Institute of Physics, Academy of Sciences of the Czech Republic, Praha, Czech Republic
- 126 Faculty of Mathematics and Physics, Charles University in Prague, Praha, Czech Republic
- 127 Czech Technical University in Prague, Praha, Czech Republic
- 128 State Research Center Institute for High Energy Physics, Protvino, Russia
- 129 Particle Physics Department, Rutherford Appleton Laboratory, Didcot, United Kingdom
- 130 Physics Department, University of Regina, Regina, SK, Canada
- 131 Ritsumeikan University, Kusatsu, Shiga, Japan
- 132 ^(a) INFN Sezione di Roma I; ^(b) Dipartimento di Fisica, Università La Sapienza, Roma, Italy
- 133 ^(a) INFN Sezione di Roma Tor Vergata; ^(b) Dipartimento di Fisica, Università di Roma Tor Vergata, Roma, Italy
- 134 ^(a) INFN Sezione di Roma Tre; ^(b) Dipartimento di Fisica, Università Roma Tre, Roma, Italy
- 135 ^(a) Faculté des Sciences Ain Chock, Réseau Universitaire de Physique des Hautes Energies – Université Hassan II, Casablanca; ^(b) Centre National de l’Energie des Sciences Techniques Nucleaires, Rabat; ^(c) Faculté des Sciences Semlalia, Université Cadi Ayyad, LPHEA-Marrakech; ^(d) Faculté des Sciences, Université Mohamed Premier and LTPM, Oujda; ^(e) Faculty of sciences, Mohammed V-Agdal University, Rabat, Morocco
- 136 DSM/IRFU (Institut de Recherches sur les Lois Fondamentales de l’Univers), CEA Saclay (Commissariat a l’Energie Atomique), Gif-sur-Yvette, France
- 137 Santa Cruz Institute for Particle Physics, University of California Santa Cruz, Santa Cruz CA, United States
- 138 Department of Physics, University of Washington, Seattle, WA, United States
- 139 Department of Physics and Astronomy, University of Sheffield, Sheffield, United Kingdom
- 140 Department of Physics, Shinshu University, Nagano, Japan
- 141 Fachbereich Physik, Universität Siegen, Siegen, Germany
- 142 Department of Physics, Simon Fraser University, Burnaby, BC, Canada
- 143 SLAC National Accelerator Laboratory, Stanford, CA, United States
- 144 ^(a) Faculty of Mathematics, Physics & Informatics, Comenius University, Bratislava; ^(b) Department of Subnuclear Physics, Institute of Experimental Physics of the Slovak Academy of Sciences, Kosice, Slovak Republic
- 145 ^(a) Department of Physics, University of Johannesburg, Johannesburg; ^(b) School of Physics, University of the Witwatersrand, Johannesburg, South Africa
- 146 ^(a) Department of Physics, Stockholm University; ^(b) The Oskar Klein Centre, Stockholm, Sweden
- 147 Physics Department, Royal Institute of Technology, Stockholm, Sweden
- 148 Departments of Physics & Astronomy and Chemistry, Stony Brook University, Stony Brook, NY, United States
- 149 Department of Physics and Astronomy, University of Sussex, Brighton, United Kingdom
- 150 School of Physics, University of Sydney, Sydney, Australia

- ¹⁵¹ Institute of Physics, Academia Sinica, Taipei, Taiwan
¹⁵² Department of Physics, Technion: Israel Inst. of Technology, Haifa, Israel
¹⁵³ Raymond and Beverly Sackler School of Physics and Astronomy, Tel Aviv University, Tel Aviv, Israel
¹⁵⁴ Department of Physics, Aristotle University of Thessaloniki, Thessaloniki, Greece
¹⁵⁵ International Center for Elementary Particle Physics and Department of Physics, The University of Tokyo, Tokyo, Japan
¹⁵⁶ Graduate School of Science and Technology, Tokyo Metropolitan University, Tokyo, Japan
¹⁵⁷ Department of Physics, Tokyo Institute of Technology, Tokyo, Japan
¹⁵⁸ Department of Physics, University of Toronto, Toronto, ON, Canada
¹⁵⁹ ^(a) TRIUMF, Vancouver BC; ^(b) Department of Physics and Astronomy, York University, Toronto, ON, Canada
¹⁶⁰ Institute of Pure and Applied Sciences, University of Tsukuba, 1-1-1 Tennodai, Tsukuba, Ibaraki 305-8571, Japan
¹⁶¹ Science and Technology Center, Tufts University, Medford, MA, United States
¹⁶² Centro de Investigaciones, Universidad Antonio Narino, Bogota, Colombia
¹⁶³ Department of Physics and Astronomy, University of California Irvine, Irvine, CA, United States
¹⁶⁴ ^(a) INFN Gruppo Collegato di Udine; ^(b) ICTP, Trieste; ^(c) Dipartimento di Chimica, Fisica e Ambiente, Università di Udine, Udine, Italy
¹⁶⁵ Department of Physics, University of Illinois, Urbana, IL, United States
¹⁶⁶ Department of Physics and Astronomy, University of Uppsala, Uppsala, Sweden
¹⁶⁷ Instituto de Física Corpuscular (IFIC) and Departamento de Física Atómica, Molecular y Nuclear and Departamento de Ingeniería Electrónica and Instituto de Microelectrónica de Barcelona (IMB-CNM), University of Valencia and CSIC, Valencia, Spain
¹⁶⁸ Department of Physics, University of British Columbia, Vancouver, BC, Canada
¹⁶⁹ Department of Physics and Astronomy, University of Victoria, Victoria, BC, Canada
¹⁷⁰ Department of Physics, University of Warwick, Coventry, United Kingdom
¹⁷¹ Waseda University, Tokyo, Japan
¹⁷² Department of Particle Physics, The Weizmann Institute of Science, Rehovot, Israel
¹⁷³ Department of Physics, University of Wisconsin, Madison, WI, United States
¹⁷⁴ Fakultät für Physik und Astronomie, Julius-Maximilians-Universität, Würzburg, Germany
¹⁷⁵ Fachbereich C Physik, Bergische Universität Wuppertal, Wuppertal, Germany
¹⁷⁶ Department of Physics, Yale University, New Haven, CT, United States
¹⁷⁷ Yerevan Physics Institute, Yerevan, Armenia
¹⁷⁸ Domaine scientifique de la Doua, Centre de Calcul CNRS/IN2P3, Villeurbanne Cedex, France

^a Also at Laboratório de Instrumentação e Física Experimental de Partículas – LIP, Lisboa, Portugal.

^b Also at Faculdade de Ciências and CFNUL, Universidade de Lisboa, Lisboa, Portugal.

^c Also at Particle Physics Department, Rutherford Appleton Laboratory, Didcot, United Kingdom.

^d Also at TRIUMF, Vancouver, BC, Canada.

^e Also at Department of Physics, California State University, Fresno, CA, United States.

^f Also at Novosibirsk State University, Novosibirsk, Russia.

^g Also at Fermilab, Batavia, IL, United States.

^h Also at Department of Physics, University of Coimbra, Coimbra, Portugal.

ⁱ Also at Università di Napoli Parthenope, Napoli, Italy.

^j Also at Institute of Particle Physics (IPP), Canada.

^k Also at Department of Physics, Middle East Technical University, Ankara, Turkey.

^l Also at Louisiana Tech University, Ruston, LA, United States.

^m Also at Department of Physics and Astronomy, University College London, London, United Kingdom.

ⁿ Also at Group of Particle Physics, University of Montreal, Montreal, QC, Canada.

^o Also at Department of Physics, University of Cape Town, Cape Town, South Africa.

^p Also at Institute of Physics, Azerbaijan Academy of Sciences, Baku, Azerbaijan.

^q Also at Institut für Experimentalphysik, Universität Hamburg, Hamburg, Germany.

^r Also at Manhattan College, New York, NY, United States.

^s Also at School of Physics, Shandong University, Shandong, China.

^t Also at CPPM, Aix-Marseille Université and CNRS/IN2P3, Marseille, France.

^u Also at School of Physics and Engineering, Sun Yat-sen University, Guanzhou, China.

^v Also at Academia Sinica Grid Computing, Institute of Physics, Academia Sinica, Taipei, Taiwan.

^w Also at Dipartimento di Fisica, Università La Sapienza, Roma, Italy.

^x Also at DSM/IRFU (Institut de Recherches sur les Lois Fondamentales de l'Univers), CEA Saclay (Commissariat à l'Energie Atomique), Gif-sur-Yvette, France.

^y Also at Section de Physique, Université de Genève, Geneva, Switzerland.

^z Also at Departamento de Física, Universidade de Minho, Braga, Portugal.

^{aa} Also at Department of Physics and Astronomy, University of South Carolina, Columbia, SC, United States.

^{ab} Also at Institute for Particle and Nuclear Physics, Wigner Research Centre for Physics, Budapest, Hungary.

^{ac} Also at California Institute of Technology, Pasadena, CA, United States.

^{ad} Also at Institute of Physics, Jagiellonian University, Krakow, Poland.

^{ae} Also at LAL, Univ. Paris-Sud and CNRS/IN2P3, Orsay, France.

^{af} Also at Department of Physics and Astronomy, University of Sheffield, Sheffield, United Kingdom.

^{ag} Also at Department of Physics, Oxford University, Oxford, United Kingdom.

^{ah} Also at Institute of Physics, Academia Sinica, Taipei, Taiwan.

^{ai} Also at Department of Physics, The University of Michigan, Ann Arbor, MI, United States.

* Deceased.